

## Article

# Isoselective Ring-Opening Polymerization of *rac*-Lactide Catalyzed by Simple Potassium Amidate Complexes Containing Polycyclic Aryl Group <sup>†</sup>

Jiahao Gao <sup>1,2</sup>, Wenjuan Zhang <sup>1,\*</sup>, Xing Wang <sup>1</sup>, Rui Wang <sup>1</sup>, Mingyang Han <sup>2</sup>, Furong Cao <sup>1,2</sup> and Xiang Hao <sup>2</sup>

<sup>1</sup> Beijing Key Laboratory of Clothing Materials R&D and Assessment, Beijing Engineering Research Center of Textile Nanofiber, School of Materials Science and Engineering, Beijing Institute of Fashion Technology, Beijing 100029, China

<sup>2</sup> Key Laboratory of Engineering Plastics and Beijing National Laboratory for Molecular Science, Institute of Chemistry, Chinese Academy of Sciences, Beijing 100190, China

\* Correspondence: zhangwj@bift.edu.cn; Tel.: +86-10-6428-8180

<sup>†</sup> Dedicated to Prof. Wen-Hua Sun on his 60th birthday.

**Abstract:** The isoselective ring-opening polymerization of *rac*-LA is a challenging goal. In this work, a series of potassium amidate complexes (**K1–K10**) were easily prepared and characterized using the <sup>1</sup>H/<sup>13</sup>C NMR spectrum. The molecular structures of potassium complexes **K2** and **K10** were determined by X-ray diffraction, which showed that both were two-dimensional coordination polymers due to the adjacent  $\pi$  interactions of the aryl. In the presence of benzyl alcohol (BnOH), all of the potassium complexes exhibited a high catalytic activity toward the ring-opening polymerization of *L*-lactide and *rac*-LA, yielding linear poly lactides capped with BnO or CH<sub>3</sub>O end groups. A significant solvent effect on the ROP of the *L*-LA was observed, with a superior efficiency in toluene than in THF and CH<sub>2</sub>Cl<sub>2</sub>. These complexes are *iso*-selective and act as active catalysts for the controlled ring-opening polymerization of *rac*-lactide, with a  $P_m$  from 0.54 to 0.76. This is a rare example of simple alkali metal complexes for the isoselective ROP of *rac*-lactide. The substituent greatly affected the monomer conversion and isoselectivities.

**Keywords:** potassium complexes; amidates; ring-opening polymerization; lactides; isoselective



**Citation:** Gao, J.; Zhang, W.; Wang, X.; Wang, R.; Han, M.; Cao, F.; Hao, X.

Isoselective Ring-Opening Polymerization of *rac*-Lactide Catalyzed by Simple Potassium Amidate Complexes Containing Polycyclic Aryl Group. *Catalysts* **2023**, *13*, 770. <https://doi.org/10.3390/catal13040770>

Academic Editor: Zhiqiang Fan

Received: 28 February 2023

Revised: 3 April 2023

Accepted: 7 April 2023

Published: 19 April 2023



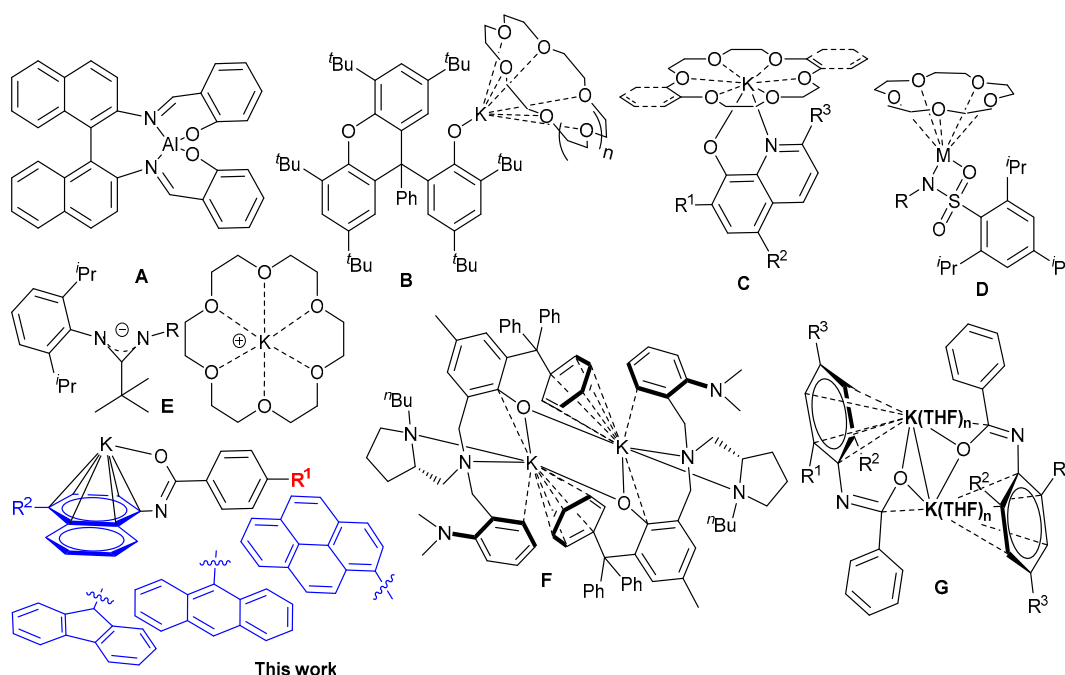
**Copyright:** © 2023 by the authors. Licensee MDPI, Basel, Switzerland. This article is an open access article distributed under the terms and conditions of the Creative Commons Attribution (CC BY) license (<https://creativecommons.org/licenses/by/4.0/>).

## 1. Introduction

Poly lactic acid (PLA), which is derived from biomass and can be completely degraded to CO<sub>2</sub> and water after use, is the representative biodegradable material at present. The most commonly used method for aliphatic polyesters is the ring-opening polymerization of cyclic esters catalyzed by metal catalysts [1–15]. However, the poor heat resistance, slow crystallization, and brittle properties of PLA materials lead to their narrow processing temperature window and limited application range [16–18]. Therefore, improvements to the heat resistance of PLA are crucial to broaden its application [19–22]. Until today, the stereocomplex PLLA, obtained by the melt blending of PDLA and PLLA in equal amounts (i.e., a melting point of the mixture of up to 230 °C), is the most effective way to improve the heat resistance of polylactide [23,24]. However, D-LA monomers or PDLA polymer are very limited and costly. Therefore, the isoselective ROP of *rac*-lactide is very attractive and also a challenging goal [25,26]. Presently, Sn(Oct)<sub>2</sub> is mostly employed for the industrial production of PLA due to its good moisture stability and solubility; however, it cannot be applied to the stereoselective ROP of *rac*-LA, as it lacks the defined and bulky stereo configuration around the active center [27,28]. Therefore, there have been many works that have focused on the design of a metal catalyst to initiate the stereoselective ROP of *rac*-LA [4,25,26,29–34].

In 1996, Spassky's group discovered the first enantiomerically pure Al complexes **A** (Scheme 1), which showed very good selectivity for the ROP of *rac*-lactides, producing

stereoblock PLA with high melting points ( $T_m = 187\text{ }^\circ\text{C}$ ) [35]. Since then, the isoselective ring-opening polymerization of *rac*-LA has become very popular, and many studies on the stereoselective ROP of *rac*-LA ( $P_m$  up to 0.99) have been realized using Al, Zn, and Y complexes bearing the special ligands that provide high-performance PLAs with good thermal stability ( $T_m > 200\text{ }^\circ\text{C}$ ), and Al complexes are the most reported [36–41]. However, the limitation of the use of aluminum complexes is the toxicity of the Al elements; for instance, aluminum derivatives are suspected to be involved in Alzheimer’s disease and have also shown a very slow polymerization rate. In order to overcome these issues, many groups have explored initiators with less toxic metals, such as magnesium and alkali metal complexes, for the ring-opening polymerization of lactides [42].



**Scheme 1.** Alkali metal complexes with conjugated structure used for the ROP of cyclic esters.

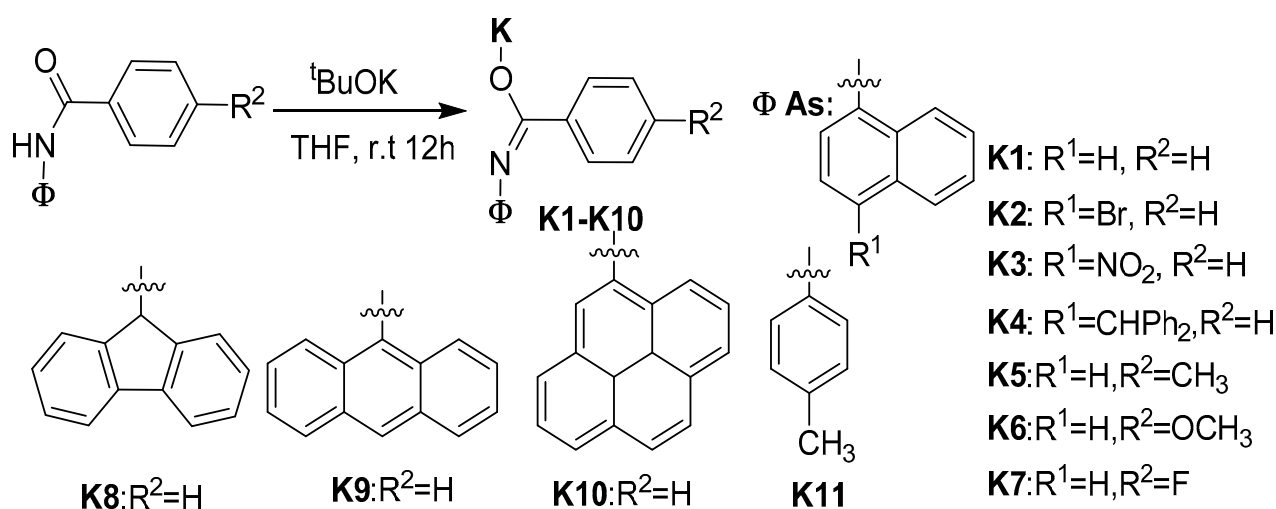
In recent years, the isoselective ROP of *rac*-lactides using crown ether alkali metal complexes have made great progress [43–49]. For example, the crown ether alkali metal complexes **B** (Scheme 1) have shown good efficiency in the ROP of *rac*-lactide, affording isotactic-enriched polylactide (PLA) [50]. Although quinolin-8-olate ligands exerted a relatively low degree of steric hindrance, the catalysts **C** still maintained stereoselective polymerization in toluene at room temperature or  $0\text{ }^\circ\text{C}$ , with the  $P_m$  ranging from 0.66 to 0.75 [48]. Moreover, the isoselectivity can also reach the high value of  $P_m = 0.84$  by using complexes **D** [47]. Ion-paired potassium amidinate complexes **E** were able to efficiently catalyze the ROP of *rac*-lactide at low temperature, and the isoselectivity reached its highest value of  $P_m = 0.88$  at  $-70\text{ }^\circ\text{C}$  [51]. These results imply that alkali metal complexes show great potential for realizing the goal of the highly active and highly stereoselective ROP of *rac*-lactide. In addition, a series of potassium complexes **F** could initiate the polymerization of *rac*-LA to achieve high monomer conversions within several minutes in the presence of *t*-PrOH, but it afforded atactic PLA with slightly isotactic-enriched microstructures [52]. Our group developed a family of sodium 2-arylimino-8-quinolates complexes that have shown good activity toward the ring-opening polymerization (ROP) of *rac*-lactide but without selectivity [53]. Recently, our group reported a series of simple potassium amidate complexes **G** that showed good efficiency for the ROP of *L*-lactides [54]. Some crystal structures, especially, clearly showed  $\pi$  interactions of the aryl with the K atom, resembling “CpM”, a sandwich form (Cp: cyclopentyl, M: metal). At the same time, the crown ether alkali metal complexes can also be regarded as “CpM” due to the similar role of the

crown ether in the “Cp”. Considering the potentially important role of the “Cp” group, in this paper, a series of potassium amidates with larger conjugated aryls were designed and evaluated for the ROP of *L*-lactides and *rac*-lactide. The crystal structure showed  $\pi$  interactions between the K and the aryl ring, and some complexes showed good activity and stereoselectivity for the ROP of *rac*-lactide. These details are discussed further in this work.

## 2. Results and Discussion

### 2.1. Synthesis and Characterization of K1–K10

A series of benzamide containing polycyclic aryls, L1–L10, were readily prepared by the reaction of the corresponding arylamines with benzoyl chloride. Compounds L1–L10 have not been reported before and hence full details of synthesis were shown in the experimental section. Treatment of L1–L10 with 2 equivalents of potassium *tert*-butoxide (KO<sup>t</sup>Bu) at ambient temperature in THF afforded the corresponding potassium complexes as solid with a good yield (Scheme 2). All complexes were characterized by <sup>1</sup>H/<sup>13</sup>C NMR spectroscopy (shown in Figures S1–S10). As a matter of course, the NMR spectra of the complexes were recorded in *d*<sub>6</sub>-DMSO because their solutions in other solvents proved to be unstable (CDCl<sub>3</sub> and *d*<sub>6</sub>-benzene). The absence of a -NH signal (around  $\delta$  10.0) in their <sup>1</sup>H NMR spectra gave support for the full conversion of L1–L10 to K1–K10 (K11 was prepared according to the literature [54]).



**Scheme 2.** Synthetic route of potassium amidates K1–K10.

The single crystal of K2 and the single crystal of K10 were obtained by laying *n*-hexane to their THF solution, and their structures were shown in Figures 1 and 2. The selected bond lengths and bond angles are shown in Tables 1 and 2. The crystal structure showed that there was a strong interaction between the K center with Aryl<sub>(N)</sub> from another molecular, which was clearly demonstrated by the bond distances [3.149–3.496 Å] of C8-K, C9-K, C11-K, C12-K, and C17-K. As shown in Figure 1, due to the interaction between the potassium with the carbon of aryl from another aryl ring, each potassium was high-coordinated by arene, one C<sub>aryl</sub>, and N from another amidate; this type of alkali metal- $\pi$  interaction has been reported in the literature on the topic several times [54]. Therefore, the molecules were packed in two-dimensional form, generating a polymeric structure (Figure 1b).

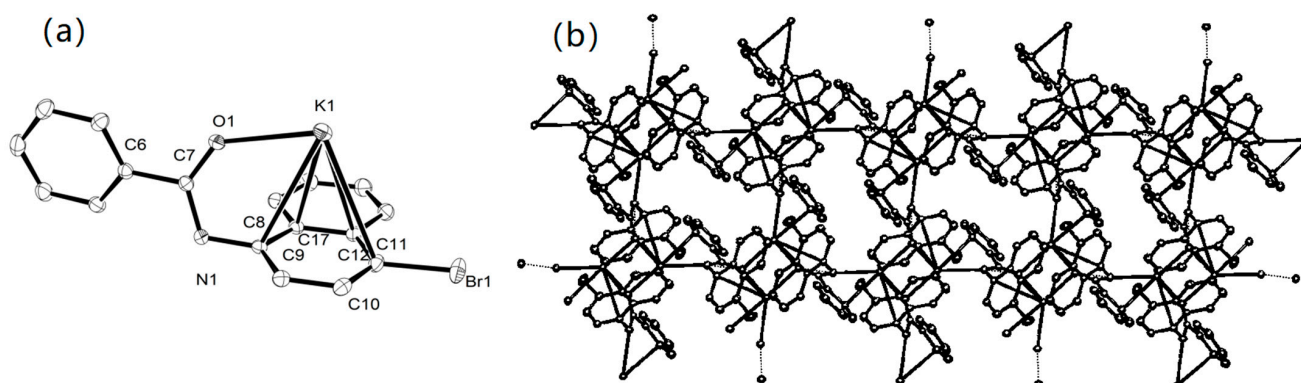


**Figure 1.** (a) Ortep drawing of structure of K2, ellipsoids are shown at the 30% probability level (left). (b) A section of the packing diagram in K2 (right).

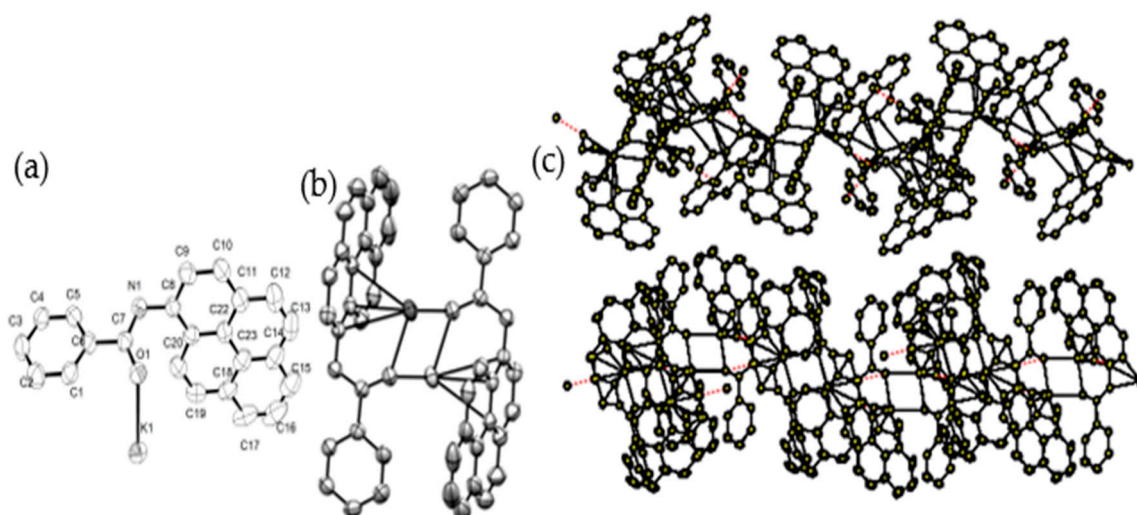


**Figure 2.** (a) Ortep drawing of structure of K10, with ellipsoids shown at the 30% probability level (left). (b) Mercury drawing dimer of K10 through interaction (middle). (c) A section of the packing diagram in K10 (right).

**Table 1.** The selected bond length and bond angles of K2 and K10.

Bond Lengths of K2 (Å)				Bond Lengths of K10 (Å)			
K1-O1	2.598(2)	K1-C11	3.413(3)	K1-O1	2.593(4)	K1-C21 <sup>3</sup>	3.058(5)
K1-O1 <sup>1</sup>	2.598(2)	K1-C12	3.232(3)	K1-N1 <sup>1</sup>	2.693(4)	K1-C22 <sup>3</sup>	3.239(5)
K1-C8	3.249(3)	K1-C17	3.149(3)	K1-C8 <sup>3</sup>	3.180(5)	K1-O1 <sup>3</sup>	2.633(4)
K1-C9	3.496(3)	K1-N1 <sup>1</sup>	2.733(2)	K1-C9 <sup>3</sup>	3.511(5)	K1-N1 <sup>4</sup>	2.693(4)
Bond angles of K2 (°)				Bond angles of K10 (°)			
O1-K1-O1 <sup>1</sup>	80.39(7)			O1-K1-K1 <sup>3</sup>	44.94(8)		
O1 <sup>1</sup> -K1-N1 <sup>1</sup>	139.25(8)			O1-K1-O1 <sup>3</sup>	89.01(11)		
O1-K1-C8	53.33(7)			O1-K1-N1 <sup>4</sup>	132.82(13)		
O1-K1-K17	64.14(7)			O1 <sup>3</sup> -K1-N1 <sup>4</sup>	111.91(12)		
O1-K1-C9	70.39(7)			O1-K1-C8 <sup>3</sup>	119.49(13)		
O1-K1-C11	102.57(7)			O1-K1-C9 <sup>3</sup>	141.63(13)		
O1-K1-C12	89.92(7)			O1-K1-C21 <sup>3</sup>	99.66(13)		
				O1-K1-C22 <sup>3</sup>	101.49(13)		

The atoms labelled superscript '1' '3' and '4' have been generated through symmetry.

The structure of K10 also showed the similar interaction between the K center with pyrene group from another molecule, in which the interaction distances of K1-C8<sup>3</sup>, K1-

C9<sup>3</sup>, K1-C21<sup>3</sup>, and K1-C22<sup>3</sup> fall in the range of 3.058~3.511 Å. However, unlike K2, these molecular chains are linked by hydrogen bonds, affording one dimension form, such as a polymeric chain.

## 2.2. Ring-Opening Polymerization of L-LA by K1–K10

To allow a suitable set of polymerization conditions to evaluate all potassium complexes, the ROP of L-LA was firstly investigated by using K2 under various conditions such as different temperature, run time, [L-LA]:[K] ratio, and solvent. The results are listed in Table 2.

When increasing the temperature from 30 °C to 50 °C, the monomer conversion using K2 was shown to increase from 42% to 96% in 15 min (runs 1–3, Table 2). The molecular weight of the polylactide (PLA) gradually increased from 0.88 to  $1.87 \times 10^4$  g mol<sup>-1</sup> while the molecular weight distribution ( $M_w/M_n$ ) became broader (from 1.73 to 2.04), suggesting more transesterification at a higher temperature [55,56]. The polymerization was then monitored between 5 min and 15 min, with the temperature maintained at 50 °C. The monomer conversion notably increased from 77% to 96% over longer run times (runs 3–5, Table 2) and the molecular weight of the PLA also increased from 1.23 to  $1.87 \times 10^4$  g mol<sup>-1</sup> but with a quite broad distribution (PDI = 1.93~2.59).

By fixing the time of 15 min and the temperature of 50 °C, the BnOH effect was investigated on the polymerization of L-LA. Without BnOH, the K2 showed good activity for ROP of L-LA with 94% conversion, similar to that (96%) with 1 equivalent BnOH, producing the PLLA with a much higher molecular weight (3.85 vs.  $1.87 \times 10^4$  g mol<sup>-1</sup>).

**Table 2.** Ring-Opening polymerization of L-lactide by K1–K10 <sup>a</sup>.

Run	Cat	LA:K:BnOH	T/°C	t/min	Solvent	Conv. <sup>b</sup> (%)	$M_{n,calcd}^c$ ( $\times 10^4$ g mol <sup>-1</sup> )	$M_n^d$ ( $\times 10^4$ g mol <sup>-1</sup> )	PDI <sup>d</sup>
1	K2	500:1:1	30	15	Toluene	42	3.06	0.88	1.73
2	K2	500:1:1	40	15	Toluene	88	6.33	1.50	1.77
3	K2	500:1:1	50	15	Toluene	96	6.93	1.87	2.04
4	K2	500:1:1	50	10	Toluene	87	6.27	1.28	1.93
5	K2	500:1:1	50	5	Toluene	77	5.59	1.23	2.59
6	K2	500:1:0	50	15	Toluene	94	6.79	3.85	1.49
7	K2	500:1:2	50	15	Toluene	100	3.62	1.05	1.74
8	K2	500:1:5	50	15	Toluene	100	1.49	0.96	1.34
9	K2	500:1:10	50	15	Toluene	100	0.73	0.87	1.32
10	K2	750:1:1	50	15	Toluene	68	7.31	3.38	1.93
11	K2	1000:1:1	50	15	Toluene	55	7.93	4.18	1.65
12	K2	1000:1:1	50	30	Toluene	59	8.48	4.52	1.79
13	K2	1000:1:1	50	60	Toluene	61	8.76	4.78	1.75
14	K2	1000:1:1	50	120	Toluene	68	9.86	6.27	1.64
15	K2	500:1:1	50	15	THF	43	3.14	7.32	1.67
16	K2	500:1:1	50	15	Hexane	0			
17	K2	500:1:1	50	15	DCM	41	2.97	5.02	1.87
18	K1	500:1:1	50	10	Toluene	78	5.61	2.20	1.70
19	K3	500:1:1	50	10	Toluene	92	6.61	1.88	1.90
20	K4	500:1:1	50	10	Toluene	71	5.11	1.45	1.54
21	K5	500:1:1	50	10	Toluene	85	6.13	2.30	1.68
22	K6	500:1:1	50	10	Toluene	95	6.85	2.46	1.81
23	K7	500:1:1	50	10	Toluene	78	5.63	1.38	1.67
24	K8	500:1:1	50	10	Toluene	73	5.30	2.34	1.63
25	K9	500:1:1	50	10	Toluene	97	7.00	1.87	1.93
26	K10	500:1:1	50	10	Toluene	82	5.94	1.70	2.02

<sup>a</sup> Conditions: 20 μmol (pre)cat., 2 mL toluene (total). <sup>b</sup> Determined by <sup>1</sup>H NMR spectroscopy. <sup>c</sup>  $M_n$  (calcd) =  $M(LA) \times \text{conversion} \times ([LA]_0/[BnOH]_0) + M_{BnOH}$ . <sup>d</sup> GPC data were recorded in THF vs. polystyrene standards using a correcting factor of 0.58 [57].

When increasing the BnOH amount to 10 equivalents, the monomer conversion was almost a 100% conversion, but the molecular weight decreased from  $3.85$  to  $0.87 \times 10^4 \text{ g mol}^{-1}$  and the molecular weight distribution was broad. All the GPC traces showed bimodal distribution and the peak of lower molecular part increased with the increase in the BnOH, indicating the chain transfer role of BnOH.

Subsequently, with the temperature kept at  $50 \text{ }^\circ\text{C}$  and the run time at 15 min, the polymerizations using **K2** were performed by varying the molar ratio of  $[\text{L-LA}]:[\text{K}]:[\text{BnOH}]$  from 500:1:1 to 1000:1:1. The results showed a sharp decrease in monomer conversion from 96% to 55% but with the molecular weight of the PLLA increasing from 1.87 to  $4.18 \times 10^4 \text{ g mol}^{-1}$  (runs 3, 10–11, Table 2), which can be explained by the higher monomer concentration favoring monomer coordination and chain propagation [58–60].

As the solvent effect was clearly observed in our previous work [54], in this work, the polymerization using **K2** was also carried out in THF, *n*-hexane, and dichloromethane. The results showed that the monomer conversion in toluene 96% was much higher than that in polar solvents ( $\text{CH}_2\text{Cl}_2$  and THF: 41–43%) (runs 3, 15, 17, Table 2). It was probably the coordination competition between the monomer and THF to K that led to the lower activity for ROP [61]. However, there was no monomer conversion in *n*-hexane (run 16, Table 2), and the reason might be the aggregation form of complexes. Indeed, the GPC traces of the PLLA in these polar solvents showed a broad distribution ( $M_w/M_n = 1.67\text{--}1.87$ ), and the molecular weight was much higher than that in toluene.

By fixing the molar ratio of  $[\text{LA}]:[\text{K}] = 500$ , all potassium complexes **K1–K10** were investigated for ring-opening polymerization of *L*-LA at  $50 \text{ }^\circ\text{C}$  within 10 min. The results showed that the substituents of  $\text{R}^1$  and  $\text{R}^2$  have a strong influence on their catalytic activity. The conversions by **K1–K4** are in the following order: **K3**( $\text{NO}_2$ ) > **K2**(Br) > **K1**(H) > **K4**( $\text{CHPh}_2$ ), suggesting that the stronger electron withdrawing group of  $\text{R}^1$  on the naphthyl led to higher activity. In contrast, another interesting point is that the stronger electron donor  $\text{R}^2$  on the *ortho*-position of acetyl benzyl will result in higher activity, which was demonstrated by the activity order: **K6** ( $\text{OCH}_3$ , 95%) > **K5** ( $\text{CH}_3$ , 85%) > **K1**(H, 78%), **K7**(F, 78%). The reason for this is probably the electron withdrawing effect. The stronger electron withdrawing group  $\text{R}^1$  on the *para*-position of naphthyl led to the lower electron density of naphthyl, which resulted in the weak interaction between the aryl group and K, and higher activity was thus achieved. However, the effect of substituent on the aryl ( $\text{C}=\text{O}$ ) was reversed. The stronger donor ability of  $\text{R}^2$  results in the stronger bond of O-K that will also weaken the interaction between the aryl group and K, and, in turn, lead to the higher activity. In addition, the molecular weight of PLLA by **K7** was much lower than by **K5**, **K6**, and **K1**. These results may be due to the easy interaction of F with the other aryl group in **K7**. The conjugated aryl ring effect was also explored by replacing the naphthyl group with flurorenyl (**K8**), anthracenyl(**K9**), and the pyrenyl group (**K10**). The results showed that potassium *N*-(anthracenyl) benzamidate **K9** showed much higher activity (97%) than that (73–82%) by **K8**, **K10**, and **K1**. All obtained polymer possessed much lower molecular weight than the calculated ones, which suggests the stronger side reaction, similar to the most of the literature on potassium complexes for the ROP of cyclic esters.

### 2.3. Microstructure Analysis of PLLA

In order to obtain more information about the mechanism of *L*-lactide polymerization, the end group of PLLA catalyzed by **K2** was analyzed by using  $^1\text{H}$  NMR and Matrix-Assisted Laser Desorption/Ionization Time of Flight Mass Spectrometry (MALDI-TOF spectrometry). When BnOH was not used, the MALDI-TOF analysis of PLLA showed that the polymer had two structural compositions, **A** and **B**, in which the peak **A** series can be attributed to linear  $(\text{C}_3\text{H}_4\text{O}_2)_n + \text{C}_3\text{H}_4\text{O}_2 + \text{CH}_3\text{OH} + \text{Na}^+/\text{K}^+$ , while **B** can be classified as cyclic  $(\text{C}_3\text{H}_4\text{O}_2)_n + \text{C}_3\text{H}_4\text{O}_2 + \text{Na}^+/\text{K}^+$  (Figure 3). The interval between the peaks of the two series were 72 Da, which is the molecular weight of half lactide, indicating that the transesterification reaction occurred during the ring-opening polymerization. At the same time, the  $^1\text{H}$  NMR spectra of the polymer showed a significant  $-\text{OCH}_3$  signal (as shown in

Figure 4), which was consistent with the results of MALDI-TOF. The methoxyl group may come from the quenching solvent of methanol [54].

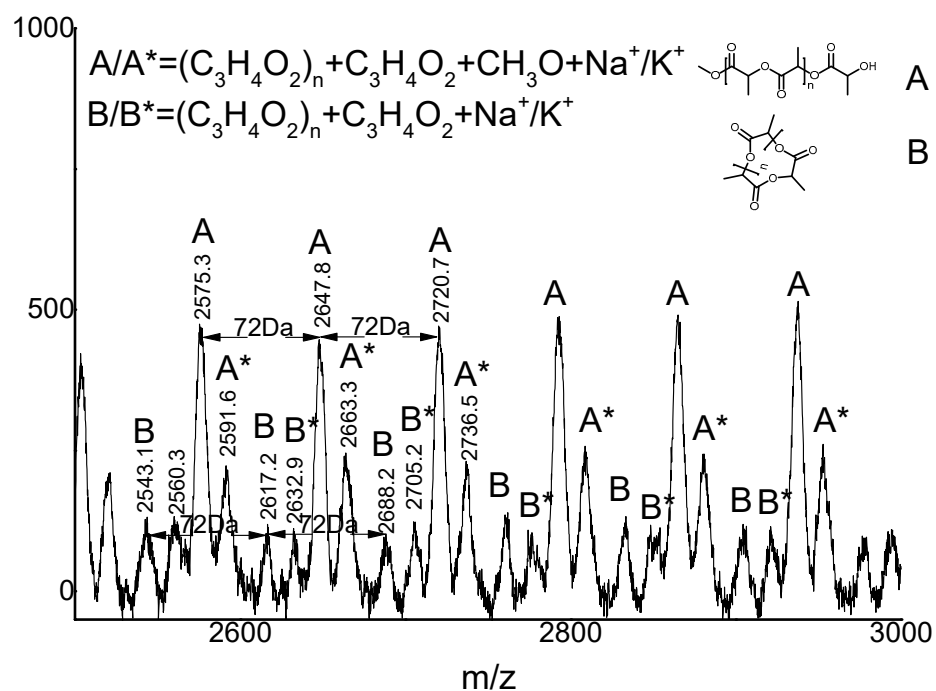


Figure 3. MALDI-TOF spectrum of poly(lactide) prepared by the ROP of *L*-LA (run 6, Table 2).

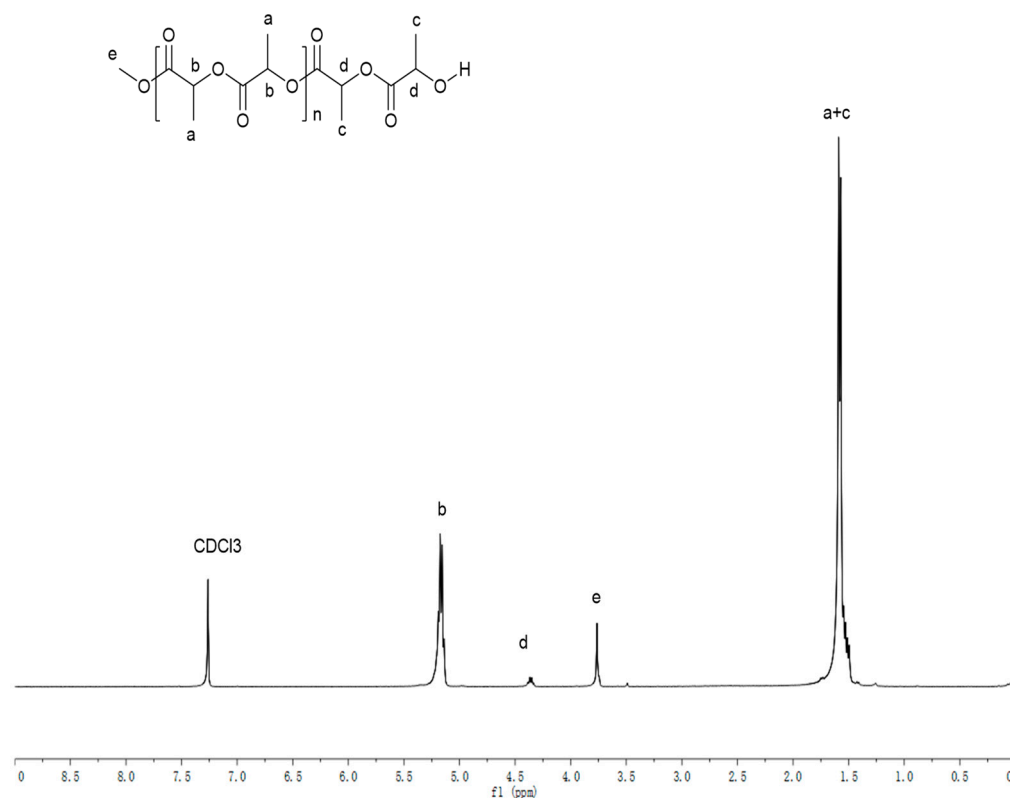


Figure 4.  $^1\text{H}$  NMR spectrum of poly(lactide) prepared by the ROP of *L*-LA (run 6, Table 2).

When one equivalent of  $\text{BnOH}$  was employed in the polymerization (run 5, Table 2), the MALDI-TOF mass spectrum showed two families of peaks, **A** and **B** (Figure S11),

in which **A** was assigned to  $(C_3H_4O_2)_n + CH_3OH + Na^+/K^+$  and **B** to  $(C_3H_4O_2)_n + PhCH_2OH + Na^+/K^+$ ; the presence of the  $PhCH_2O$  protons and  $CH_3O$  protons in this polymer were confirmed by  $^1H$  NMR spectrum (Figure S12). Evidently, intermolecular transesterification is operational in the case of the **A** and **B** series. Moreover, when two equivalent BnOH was employed (run 7, Table 2), two families of peaks were observed (Figure S13), in which **A** was assigned as  $(C_3H_4O_2)_n + CH_3OH + Na^+/K^+$  and **B** to  $(C_3H_4O_2)_n + PhCH_2OH + Na^+/K^+$ , and the  $^1H$  NMR spectrum confirmed the presence of the BnOH methylene protons and the  $CH_3O$  protons (Figure S14). In order to make the mechanism clearer, 5 equivalent and 10 equivalent benzyl alcohols were added to the reaction. The MALDI-TOF mass spectrum of resulting polymers showed two families of peaks, **A** and **B**, in which **A** was assigned to  $(C_3H_4O_2)_n + PhCH_2OH + K^+/Na^+$  and **B** to  $(C_3H_4O_2)_n + CH_3OH + K^+/Na^+$  (Figure 5), and the presence of the  $PhCH_2O$  protons and the  $CH_3O$  protons in this polymer were confirmed in the  $^1H$  NMR spectrum (Figure 6).

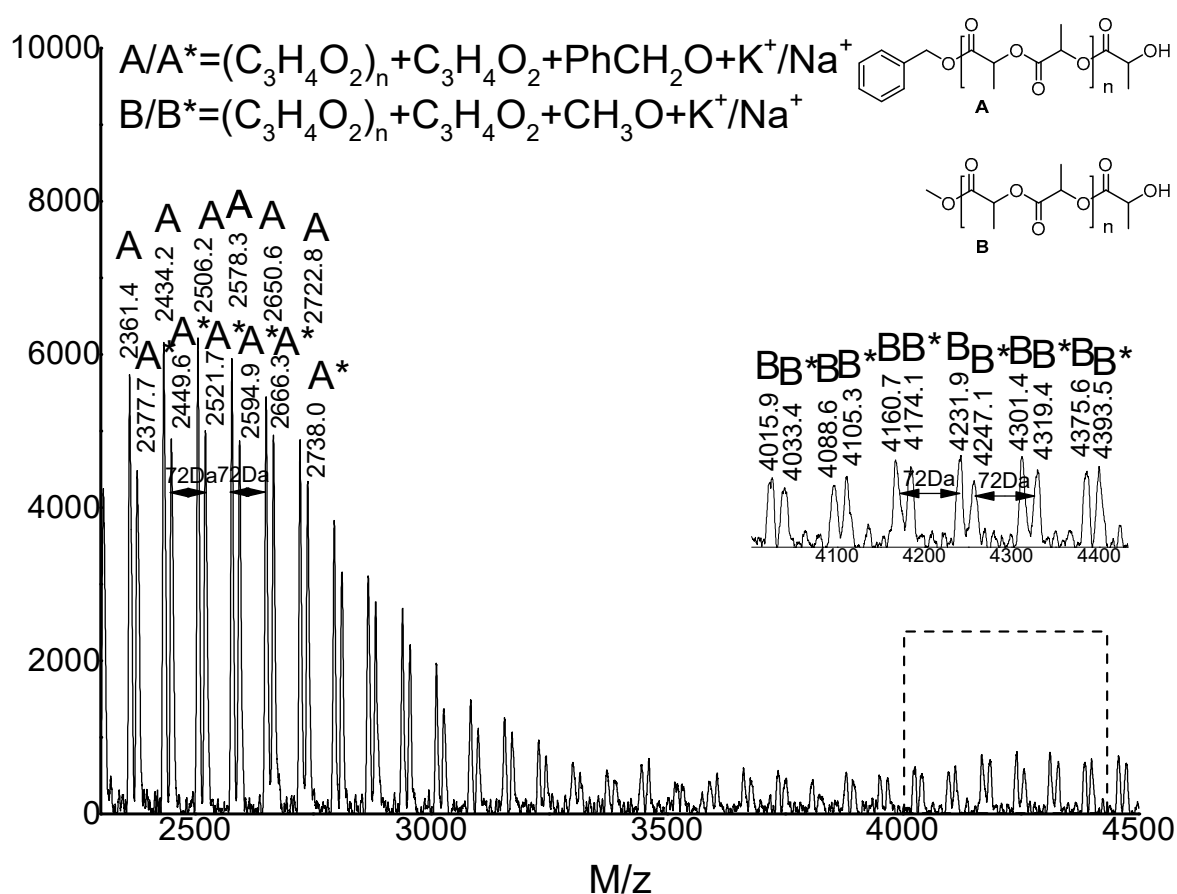


Figure 5. MALDI-TOF spectrum of PLLA obtained by K2 and 10 equiv. BnOH (run 9, Table 2).

Collectively, the results observed using K2 in the *L*-LA polymerizations that are described above suggest that two mechanisms were involved (as shown in Scheme 3), similar to previous reports [34,42,54,62,63]. One is that the K2 directly initiate the ring-opening polymerization of *L*-LA, in which the  $CH_3O$ - end group originated from the methanol used to terminate the polymerization. Conversely, the other one followed the “monomer activated mechanism (BnOH)” seen for most alkali metal systems [64–66], in which *L*-LA can be activated following coordination to the metal center and is then ring-opened via the nucleophilic attack of the benzyl alkoxide. When more BnOH was employed in the catalytic system, polymerizations preferred to proceed in Path 2, producing the linear PLLA (B/B\* family).

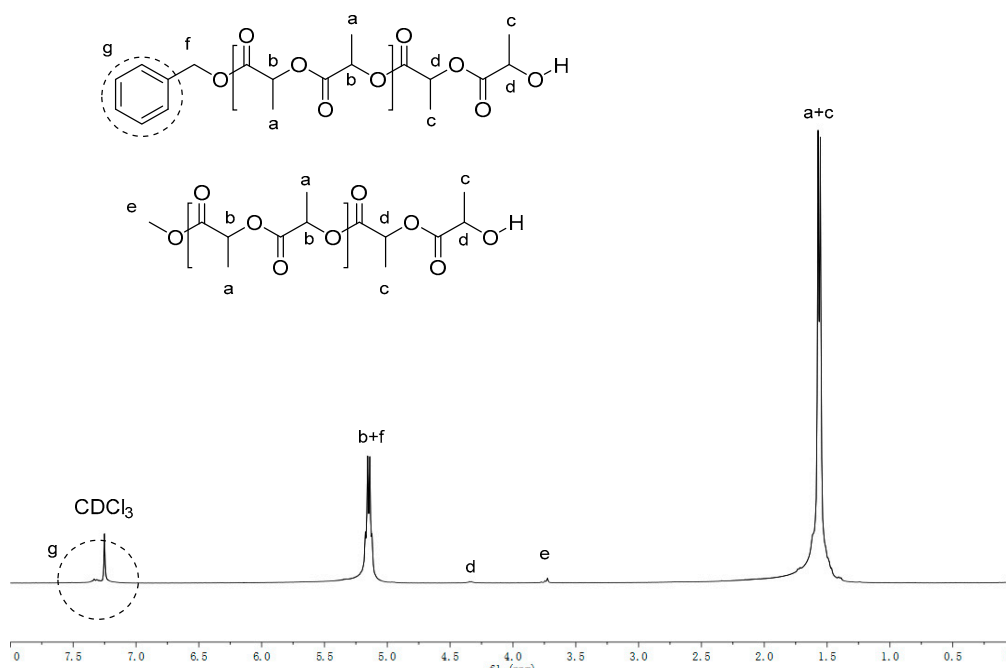
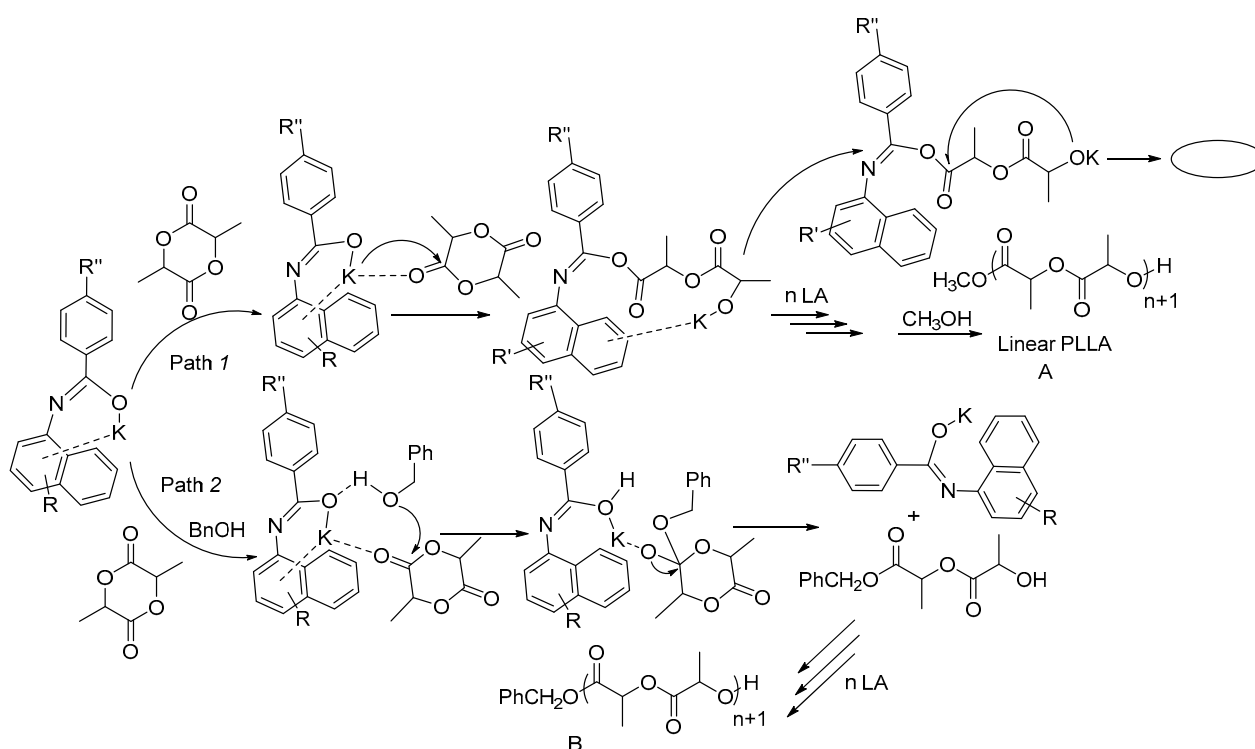


Figure 6. MALDI-TOF spectrum of PLLA prepared by **K2** and 10 equivalent BnOH (run 9, Table 2).



Scheme 3. Possible mechanisms for the ROP of *L*-LA using **K2**/BnOH.

#### 2.4. Ring-opening Polymerization of *rac*-Lactide by **K1–K11**

##### 2.4.1. Polymerization Results of *rac*-LA in 60 min

As they displayed very good activity for the ROP of *L*-LA, their selectivity toward ring-opening polymerization of *rac*-lactide was also investigated, and the results are listed in Table 3. Considering the high molar ratio of monomer to K can lead to poor controllability in polymerization, the ROP of *rac*-LA was first investigated by using **K2**/BnOH at  $[rac\text{-LA}]/K = 100$  and room temperature. The results showed 100 equivalent *rac*-lactide can be fully converted into polymer by **K2** at 20 °C in 60 min. If polymerization

temperature decreased to 0 °C, the conversion decreased to 85%. Further decreasing the temperature to −30 °C and −78 °C, there was no significant change of monomer conversion (83~85%) in 60 min (runs 3, 5, 8, Table 3). However, without BnOH, the conversion sharply decreased to 26% in 60 min at −78 °C, even extending the reaction time to 2 h, and only a 50% conversion rate could be achieved (run 11, Table 3). In addition, the obtained polymer possessed very broad distribution (PDI = 4.52 (120 min) and 3.89 (60 min)).

**Table 3.** Ring-opening polymerization of *rac*-lactide <sup>a</sup>.

Run	Cat	LA:K:BnOH	T/°C	t/min	Solvent	Conv. <sup>b</sup> (%)	$M_{n,calcd}^c$ ( $\times 10^4$ g mol <sup>−1</sup> )	$M_n^d$ ( $\times 10^4$ g mol <sup>−1</sup> )	PDI <sup>d</sup>	$P_m^e$
1	K2	100:1:1	20	60	Toluene	100	1.45	0.64	2.10	
2	K2	250:1:1	20	60	Toluene	77	2.78	1.27	1.81	
3	K2	100:1:1	0	60	Toluene	85	1.24	0.43	2.23	
4	K2	100:1:1	0	120	Toluene	100	1.45	0.61	1.85	
5	K2	100:1:1	−30	60	Toluene	85	1.23	0.45	2.03	
6	K2	100:1:1	−78	5	Toluene	54	0.78	0.26	1.79	0.76
7	K2	100:1:1	−78	10	Toluene	67	0.97	0.43	1.35	0.75
8	K2	100:1:1	−78	60	Toluene	83	1.21	0.58	1.72	0.61
9	K2	100:1:1	−78	120	Toluene	88	1.28	0.65	2.12	
10	K2	100:1:0	−78	60	Toluene	26	0.38	0.38	4.52	
11	K2	100:1:0	−78	120	Toluene	50	0.72	0.48	3.89	
12	K2	100:1:2	−78	60	Toluene	54	0.79	0.25	1.33	
13	K2	100:1:1	−78	60	hexane	54	0.79	0.56	1.41	0.58
14	K2	100:1:1	−78	60	THF	56	0.82	0.86	1.58	0.67
15	K2	100:1:1	−78	60	DCM	64	0.93	0.79	1.67	0.64
16	K1	100:1:1	−78	60	Toluene	95	1.38	1.21	1.91	0.59
17	K3	100:1:1	−78	60	Toluene	95	1.38	0.87	1.24	0.54
18	K4	100:1:1	−78	60	Toluene	82	1.19	1.23	1.17	0.67
19	K5	100:1:1	−78	60	Toluene	68	0.99	0.81	1.99	0.60
20	K6	100:1:1	−78	60	Toluene	83	1.21	0.75	1.83	0.61
21	K7	100:1:1	−78	60	Toluene	78	1.13	0.93	1.65	0.61
22	K8	100:1:1	−78	60	Toluene	67	0.97	0.66	1.21	0.56
23	K9	100:1:1	−78	60	Toluene	94	1.36	0.61	1.42	0.65
24	K10	100:1:1	−78	60	Toluene	85	1.23	0.60	1.56	0.68
25	K11 <sup>f</sup>	100:1:1	−78	60	Toluene	63	0.92	0.63	1.69	0.54

<sup>a</sup> Conditions: 20 μmol (pre)cat., 1 mL toluene (total). <sup>b</sup> Determined by <sup>1</sup>H NMR spectroscopy. <sup>c</sup>  $M_n$  (calcd) =  $M(LA) \times \text{conversion} \times ([LA]_0/[BnOH]_0) + M_{BnOH}$ . <sup>d</sup> GPC data were recorded in THF vs. polystyrene standards using a correcting factor of 0.58 [57]. <sup>e</sup> Determined by homonuclear-decoupled <sup>1</sup>H NMR spectroscopy. <sup>f</sup> This complex is from our previous work [54].

At −78 °C, the ROP of *rac*-LA were then investigated from 5 to 120 min, and the results showed conversion gradually increased from 54% to 88%, with molecular weight also increasing from 0.26 to  $0.65 \times 10^4$  g mol<sup>−1</sup> (runs 6–9, Table 3). Especially from 60 to 120 min, there was a slight increase in monomer conversion from 83% to 88%. It is very interesting that the  $P_m$  values decreased from 0.76 to 0.61, indicating the selectivity decreased due to more side reaction of transesterification in a longer time. Complex K2, iso-selectivities of  $P_m = 0.76$  (Figure 7) and 0.75 (Figure S28), were achieved when the ratios of  $[rac\text{-lactide}]_0:[K2]_0:[BnOH]_0$  were 100:1:1 with 5 min or 10 min, respectively, in toluene at −78 °C (runs 6, 7 in Table 3).

The solvent effect was also investigated within 60 min. The results showed that conversion (54~56%) in other solvents such as hexane, THF, or dichloromethane are much lower than (83%) in toluene (runs 8, 13–15, Table 3). However, the isoselectivity in THF ( $P_m = 0.67$ ) or dichloromethane ( $P_m = 0.64$ ) are both higher than in the toluene ( $P_m = 0.61$ ), suggesting the polarity of the solvent effect on stereoselectivity toward the ROP of *rac*-LA.

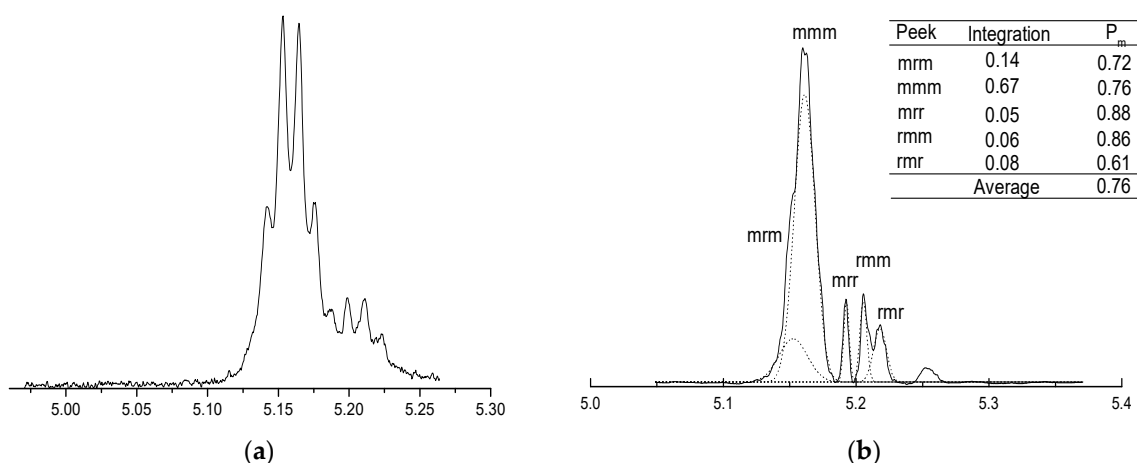


**Figure 7.** (a)  $^1\text{H}$  NMR spectrum of *rac*-LA obtained by **K2** (run 6, Table 3); (b) Homonuclear-decoupled  $^1\text{H}$  NMR spectroscopy of *rac*-LA obtained by **K2** (run 6, Table 3). The  $P_m$  values were determined for all tetrads based on Bernoulli statistics, and their average value was used.

In order to better investigate the effect of different substituents on the polymerization selectivity, we studied the catalytic properties of different catalysts for *rac*-lactide at  $-78\text{ }^\circ\text{C}$  and 60 min. Generally, all these complexes **K1–K10** showed better activity than **K11** bearing phenyl ring, which to some extent indicates that the bigger conjugated aryl ring may help to increase activity. Among those complexes, **K1**, **K3**, and **K9** showed good catalytic activity with over 90% conversion, much higher than other complexes. In contrast, **K5** and **K8** exhibited much lower activity (conversion 67–68%) than others. All the obtained polymers have much lower molecular weights than those calculated, indicating that the polymerization reaction is less controllable. The isoselectivities of ROP of *rac*-LA were also greatly influenced by the substituents. **K9**, **K10**, and **K4** showed much better selectivity with  $P_m$  values (0.65–0.68) than others ( $P_m$  ranging 0.54–0.61). The reason is probably the bigger  $\pi$ -conjugated aryl group of anthracenyl (**K9**), as the pyrenyl group (**K10**) favor the monomeric potassium species generation and act as a “CpM” model to influence the coordination of different monomer coordination and insertions. The polymer by **K8** and **K3** showed almost no selectivity with low  $P_m$  values (0.54 and 0.56). The reason may be due to the fluorenyl group of non-conjugated aryl ring that could not support the monomeric “CpM” form of **K8** and thus led to the poor selectivity. While for **K3** containing the strong electron withdrawing group of  $\text{NO}_2$ , the reason is that they are very easy to form one-dimension polymeric potassium complexes, as in our previous report without  $\pi$ -interaction of K with aryl ring, and this thus led to poor selectivity. Similar to our previous report that the potassium containing  $\text{NO}_2$  group exhibited good activity for ROP of *L*-LA [54], in this case, **K3** also exhibited much better activity for ROP of *rac*-LA than others. Complex (**K4** and **K10**) showed higher selectivity ( $P_m = 0.67$ ) than other complexes (**K6**, **K7**, **K8**) ( $P_m = 0.59$ –0.61).

#### 2.4.2. Results of ROP toward *rac*-LA in 5 min

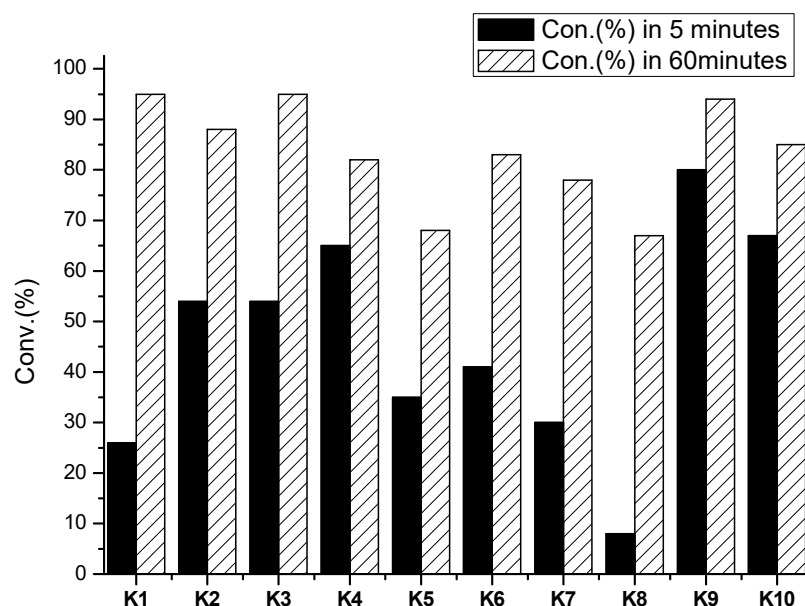
Due to the longer time increasing the occurrence of transesterification and lowering the selectivity, and in order to more clearly clarify the substituent effect of potassium complexes on the selectivity of ROP of *rac*-LA, all potassium complexes **K1–K10** were further investigated for the ROP of *rac*-LA in the short time of 5 min and results were collected in Table 4.

**Table 4.** Ring-opening polymerization of *rac*-lactide <sup>a</sup>.

Run	Cat	LA:K:BnOH	Conv(%) <sup>b</sup>	Mn <sub>Calcd</sub> <sup>c</sup>	Mn <sup>d</sup>	PDI <sup>d</sup>	P <sub>m</sub> <sup>e</sup>
1	K1	100:1:1	26	0.38	0.19	1.13	0.66
2	K2	100:1:1	54	0.78	0.26	1.79	0.76
3	K3	100:1:1	54	0.78	0.89	1.44	0.65
4	K4	100:1:1	65	0.94	0.61	1.83	0.68
5	K5	100:1:1	35	0.51	0.39	1.77	0.66
6	K6	100:1:1	41	0.60	0.29	1.34	0.67
7	K7	100:1:1	30	0.44	0.46	1.82	0.63
8	K8	100:1:1	8	0.12	0.29	1.32	0.61
9	K9	100:1:1	80	1.16	0.37	1.45	0.72
10	K10	100:1:1	67	0.97	0.29	1.07	0.72

<sup>a</sup> Conditions: 20 μmol (pre)cat., 1 mL toluene (total), 5 min, −78 °C, <sup>b</sup> Determined by <sup>1</sup>H NMR spectroscopy. <sup>c</sup>  $M_n$  (calcd) =  $M(LA) \times \text{conversion} \times ([LA]_0/[BnOH]_0) + M_{BnOH}$ . Unit:  $\times 10^4 \text{ g mol}^{-1}$ , <sup>d</sup> GPC data were recorded in THF vs. polystyrene standards using a correcting factor of 0.58 [57]. <sup>e</sup> Determined by homonuclear-decoupled <sup>1</sup>H NMR spectroscopy.

As shown in Figure 8, generally, the conversions by **K1–K10** in 5 min were much lower than that in 10 min, indicating that the longer time increased the monomer conversion. It is very interesting to see that the **K9** bearing anthracenyl group exhibited the highest activity toward the ROP of *rac*-LA in 5 min, with more than 80% conversion. The **K10** bearing pyrenyl group, meanwhile, showed lower activity than **K9**, but still a much higher (conv. 67%) conversion than the **K1–K7** bearing naphthyl group (conv. 26–65%), whilst **K8** exhibited the lowest activity with only a 8% conversion in 5 min, the same activity order to its result in 60 min. On the other hand, these results further illustrated the bigger pi-conjugated **K9**, and **K10** can quickly initiate the ring-opening polymerization of *rac*-LA, while the **K1–K7** containing naphthyl group gradually initiated the polymerization.

**Figure 8.** Comparing the conversion by **K1–K10** in 5 or 60 min.

As the substituent of potassium complexes greatly affected their polymerization activity, their influence on isoselectivity toward ROP of *rac*-LA was also investigated. We found that, generally, the isoselectivity of PLA in 5 min were much better ( $P_m$ : 0.61–0.76) than that obtained in 60 min ( $P_m$ : 0.54–0.68) (shown in Figure 9), which may be due to the increasing side reaction in the longer time.

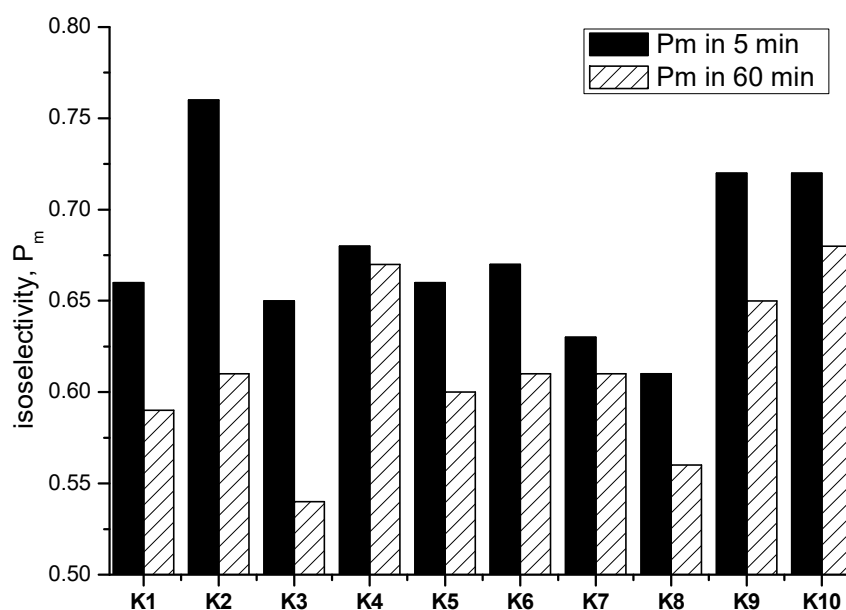


**Figure 9.** Comparing the isoselectivity of ROP by K1–K10 in 5 or 60 min.

Figure 9 also showed that the isoselectivity changes depended on the substituent. For K4 containing the very bulky group of dibenzhydryl on naphthyl, there was almost no change of  $P_m$  values (from 0.68 to 0.67), indicating that the bulky substituent greatly affected the geometry of active species and suppressed the side reaction of transesterification. In addition, another interesting thing to note is that the bigger conjugated aryl substituted potassium complexes exhibited better isoselectivity toward the ring-opening polymerization of *rac*-LA, which was demonstrated by the  $P_m$  values in 5 min:  $K9_{(An)} \approx K10_{(Pyrene)} > K1_{(Quin)} > K8_{(Flu)}$ . Within the longer time of 60 min, K9, K10 still showed better isoselectivity than K1, K8, further indicating that the higher conjugated aryl ring favor the selectivity. Within 5 min, the  $R^2$ -substituted *N*-naphthalenyl benzimidate potassium complexes showed similar selectivity ( $P_m = 0.63\sim 0.66$ ) towards the ROP of *rac*-LA, with the slight trend of  $K6_{(OCH_3)} > K5_{(CH_3)} > K1_{(H)} > K7_{(F)}$ , indicating a little electronic effect by *p*-substituent on the aryl.

As is well documented, the physical, mechanical, and degradation properties of polylactide are intimately related to chain stereochemistry. Typically, isotactic PLLA is a highly crystalline material with a  $T_m \approx 170.0$  °C, whereas atactic poly(*D, L*)-LA is amorphous without a clear  $T_m$  [26,67]. Hence, melting transition temperatures have been used to characterize the stereoregularity of polylactides to some extent. The DSC curves of polymer obtained by K2, K3, K8, and K10 in 5 min showed that they have an obvious melting point with  $T_m$  values from 130~172 °C (shown in Figure S29), indicating that all of them are crystalline polymers, which is in line with their isotactic selectivity.

### 3. Experimental Section

#### 3.1. General Procedures

All manipulations were performed under high purity nitrogen with a rigorous exclusion of air and moisture using standard Schlenk techniques or glove-boxes. Toluene, n-hexane, diethyl ether, and THF were dried over sodium benzophenone under reflux and then distilled under nitrogen, and finally stored over activated molecular sieves (4 Å) for 24 h in a glove-box prior to use. *L*-LA was provided by TCI (Tokyo Chemical Industry, Tokyo, Japan). <sup>t</sup>BuOK was purchased from J&K Scientific (Beijing, China) and used as received. BnOH was provided by Aldrich (Tokyo, Japan). Naphthylamine, 4-brominated naphthalamide, 9-aminofluorene hydrochloride, and 9-nitroanthracene were provided by Ark Pharm(Shanghai, China). 1-pyrenamine was provided by TCI (Tokyo, Japan). 4-nitronaphthylamine, diphenylmethanol, 4-methylbenzoyl chloride, and 4-methoxybenzoyl

chloride 4-fluorobenzoyl chloride were provided by J&K Scientific (Beijing, China). Differential scanning calorimetry (DSC, TA2000) was performed under a nitrogen atmosphere to record the melting temperatures of the polyethylenes. The testing program was set as follows: a sample (4.0–6.0 mg) was heated to 200 °C at a heating rate of 20 °C per min for 5 min at the same temperature to remove its thermal history and then cooled to –50 °C at the same heating rate. Elemental analysis was carried out with a Flash EA 1112 microanalyzer. The  $^1\text{H}$  and  $^{13}\text{C}$  NMR spectra were recorded on a Bruker DMX-400 instrument. The MALDI-TOF spectra was recorded on Bruker autoflex III by the linear positive ion method. The GPC measurements were performed using a system composed of a 390-LC multidetector (MDS), 209-LC pump injection module (PIM), and a PL-GPC 50 plus instrument. THF was used as the eluent (flow rate: 1.0 mL/min, at 40 °C) and the molecular weights and molecular weight distributions were calculated using polystyrene as the standard.

### 3.2. Synthesis and Characterization of L1–L10

**Synthesis of *N*-naphthalen benzamide (L1):** Naphthylamine (1.43 g, 10 mmol) was added to a 100 mL round-bottom flask and dissolved in 50 mL of dichloromethane. The resulting solution was stirred for 10 min with a subsequent dropwise addition of benzoyl chloride (4.20 g, 30 mmol). The reaction was stirred for about 9 h. After it was filtered, the white solid was obtained, and washed with anhydrous diethyl ether. Yield: 0.90 g, 36%.  $^1\text{H}$  NMR (400 MHz,  $d_6$ -DMSO, TMS):  $\delta$  10.41 (s, 1 H), 8.08 (d,  $J$  = 8.0 Hz, 2 H), 7.96 (s, 2 H), 7.85 (d,  $J$  = 8.0 Hz, 2 H), 7.62–7.52 (m, 7 H);  $^{13}\text{C}$  NMR (100 MHz,  $d_6$ -DMSO, TMS): 134.1, 129.6, 128.7, 127.8, 127.3, 126.7, 125.9, 122.4, 120.2.

**Synthesis of *N*-(4-bromonaphthalen-1-yl)benzamide (L2):** The experimental method described for L1 was used in the preparation of L2 but using 4-brominated naphthalamide (1.11 g, 5.0 mmol) and benzoyl chloride (2.10 g, 15 mmol). White solid was obtained. Yield: 0.79 g, 48%.  $^1\text{H}$  NMR (400 MHz,  $d_6$ -DMSO, TMS):  $\delta$  10.53 (s, 1 H), 8.19 (d,  $J$  = 8.0 Hz, 1 H), 8.08 (t,  $J$  = 4.0 Hz, 3H), 7.94 (d,  $J$  = 8.0 Hz, 1 H), 7.74 (t,  $J$  = 8.0 Hz, 1 H), 7.68–7.59 (m, 2 H), 7.57 (t,  $J$  = 4.0 Hz, 3H);  $^{13}\text{C}$  NMR (100 MHz,  $d_6$ -DMSO, TMS): 166.5, 134.5, 134.4, 132.0, 130.7, 129.9, 128.7, 128.2, 128.0, 127.2, 126.9, 124.8, 124.4, 119.5.

**Synthesis of *N*-(4-nitronaphthalen-1-yl)benzamide (L3):** The experimental method described for L1 was used in the preparation of L3 using 4-nitronaphthylamine (0.99 g, 5 mmol) and benzoyl chloride (2.10 g, 15 mmol). White solid was obtained. Yield: 0.63 g, 43%.  $^1\text{H}$  NMR (400 MHz,  $d_6$ -DMSO, TMS):  $\delta$  9.03 (d,  $J$  = 8.0 Hz, 1 H), 8.94 (s, 1 H), 7.77 (d,  $J$  = 8.0 Hz, 1 H), 8.74 (d,  $J$  = 8.0 Hz, 1 H), 8.69 (t,  $J$  = 8.0 Hz, 1 H), 8.31 (d,  $J$  = 8.0 Hz, 1 H), 8.26 (d,  $J$  = 8.0 Hz, 1 H), 7.94–7.85 (m, 3 H), 7.72 (t,  $J$  = 8.0 Hz, 1 H);  $^{13}\text{C}$  NMR (100 MHz,  $d_6$ -DMSO, TMS): 167.5, 147.4, 136.1, 134.2, 132.0, 129.4, 128.8, 127.5, 126.6, 126.3, 123.5, 121.5, 117.6.

**Synthesis of *N*-(4-dibenzhydrylnaphthalen-1-yl) benzamide (L4):** Step 1: A mixture of naphthylamine (4.2 g, 30 mmol), diphenylmethanol (6.7 g, 60 mmol), and a catalytic amount of zinc chloride (0.52 g, 4.0 mmol) in HCl (20 mL) was refluxed for 3 h. After solvent evaporation at reduced pressure, the residue was purified by column chromatography on basic alumina with the eluent of petroleum ether and ethyl acetate (v:v = 30:1) to afford a purple solid in 60% isolated yield.  $^1\text{H}$  NMR: (400 MHz,  $\text{CDCl}_3$ , TMS):  $\delta$  7.95 (d,  $J$  = 8 Hz, 1 H), 7.86 (d,  $J$  = 8 Hz, 1 H), 7.45–7.37 (m, 2 H), 7.25 (d,  $J$  = 8 Hz, 5 H), 7.20 (t,  $J$  = 8 Hz, 2 H), 7.12 (d,  $J$  = 8 Hz, 5 H), 6.75–6.70 (m, 2 H), 6.18 (s, 1 H).

Step 2: The 4-dibenzhydrylnaphthalen (0.23 g, 1 mmol) was added to a 50 mL round-bottom flask dissolved in 10 mL of toluene. The resulting solution was stirred for 10 min with a subsequent dropwise addition of benzoyl chloride (0.40 g, 2.0 mmol). The reaction was stirred about 8h at 80 °C. After it was filtered, the filtrate, a yellow solid, was obtained, and it was washed with anhydrous ether. Yield: 0.30 g, 63%.  $^1\text{H}$  NMR: (400 MHz,  $d_6$ -DMSO, TMS):  $\delta$  10.39 (s, 1 H, N-H), 8.13–8.05 (m, 3 H, Ar-H), 8.02–7.98 (m, 1 H, Ph-H), 7.62–7.45 (m, 6 H, Ar-H), 7.33 (t,  $J$  = 8.0 Hz, 4 H, Ar-H), 7.23 (t,  $J$  = 8.0 Hz, 2H, Ar-H), 7.15 (d,  $J$  = 8.0 Hz, 4 H, Ph-H), 6.73 (d,  $J$  = 8.0 Hz, 1 H, Ar-H), 6.44 (s, 1 H, Ar-H).

**Synthesis of 4-methyl-*N*-(naphthalen-1-yl) benzamide (L5):** The naphthylamine (2.8 g, 20 mmol) was added to a 50 mL round-bottom flask dissolved in 30 mL of toluene. The resulting solution was stirred for 10 min with a subsequent dropwise addition of 4-methylbenzoyl chloride (3.98 g, 25.8 mmol). The reaction was stirred for about 8 h at 80 °C. After it was filtered, a white solid was obtained and washed with anhydrous ether. Yield: 1.95 g, 53%. <sup>1</sup>H NMR: (400 MHz, *d*<sub>6</sub>-DMSO, TMS): δ 10.37 (s, 1 H, N-H), 8.11 (d, *J* = 8 Hz, 2 H, Ar-H), 7.99–7.95 (m, 1 H, Ar-H), 7.90 (d, *J* = 8 Hz, 1 H, Ph-H), 7.85 (d, *J* = 8 Hz, 1 H, Ph-H), 7.68–7.59 (m, 4 H, Ar-H), 7.36 (d, *J* = 8 Hz, 2 H, Ph-H), 2.41 (s, 3 H, CH<sub>3</sub>). <sup>13</sup>C NMR: (100 MHz, *d*<sub>6</sub>-DMSO, TMS): δ 166.5, 142.1, 134.2, 132.1, 129.5, 128.8, 128.3, 127.4, 125.2, 125.1, 122.5, 21.5.

**Synthesis of 4-methoxy-*N*-(naphthalen-1-yl) benzamide (L6):** The naphthylamine (2.1 g, 15 mmol) was added to a 250 mL round-bottom flask and dissolved in 30 mL toluene. The resulting solution was stirred for 10 min with a subsequent dropwise addition of 4-methoxybenzoyl chloride (2.8 g, 16.4 mmol). The reaction was stirred for about 8 h at room temperature. After it was filtered, the filtrate, a white solid, was obtained, and it was washed with anhydrous ether. Yield: 1.54 g, 77%. <sup>1</sup>H NMR: (400 MHz, *d*<sub>6</sub>-DMSO, TMS): δ 10.27 (s, 1 H, N-H), 8.09 (d, *J* = 8 Hz, 2 H, Ar-H), 7.98 (d, *J* = 8 Hz, 2 H, Ph-H), 7.85 (d, *J* = 8 Hz, 1 H, Ar-H), 7.59–7.53 (m, 4 H, Ar-H), 7.09 (d, *J* = 8 Hz, 2 H, Ph-H), 3.86 (s, 3 H, OCH<sub>3</sub>). <sup>13</sup>C NMR: (100 MHz, *d*<sub>6</sub>-DMSO, TMS): δ 166.0, 162.4, 134.6, 134.2, 130.2, 129.8, 127.1, 126.6, 126.5, 126.3, 126.0, 124.4, 123.9, 114.1, 55.9.

**Synthesis of 4-fluoro-*N*-(naphthalen-1-yl) benzamide (L7):** The naphthylamine (2.1 g, 15 mmol) was added to a 250 mL round-bottom flask dissolved in 30 mL of toluene. The resulting solution was stirred for 10 min with a subsequent dropwise addition of 4-fluorobenzoyl chloride (2.8 g, 17 mmol). The reaction was stirred for about 4 h at 80 °C. After it was filtered, the filtrate, a white solid, was obtained, and it was washed with anhydrous ether. Yield: 1.49 g, 37.4%. <sup>1</sup>H NMR: (400 MHz, *d*<sub>6</sub>-DMSO, TMS): δ 10.32 (s, 1 H, N-H), 8.12 (d, *J* = 8 Hz, 2 H, Ar-H), 8.01 (d, *J* = 8 Hz, 2 H, Ph-H), 7.85 (d, *J* = 8 Hz, 1 H, Ar-H), 7.62–7.53 (m, 4 H, Ar-H), 7.11 (d, *J* = 8 Hz, 2 H, Ph-H). <sup>13</sup>C NMR: (100 MHz, *d*<sub>6</sub>-DMSO, TMS): δ 168.3, 165.1, 137.6, 137.9, 137.8, 126.6, 126.3, 125.8, 124.7, 122.5, 122.1, 121.6, 120.4, 117.2.

**Synthesis of *N*-(9H-fluoren-9-yl)benzamide (L8):** Step 1: 9-aminofluorene hydrochloride (1.27 g, 5.0 mmol) was added to a 100 mL round-bottom flask, dissolved in 10 mL of acetic acid. Adjusting the pH of solvent into pH = 7 with 5% NaOH, excess solvent was removed in a vacuum. 20 mL DCM was added to the flask and stirred for 30 min. The white solid was obtained after it was filtered. Yield: 0.99 g, 91%. <sup>1</sup>H NMR (400 MHz, *d*<sub>6</sub>-DMSO, TMS): δ 9.24 (s, 1 H), 8.03 (d, *J* = 8.0 Hz, 2 H), 7.92 (d, *J* = 8.0 Hz, 2 H), 7.52 (t, *J* = 8.0 Hz, 2 H), 7.41 (t, *J* = 8.0 Hz, 2 H), 5.38 (s, 1 H)

Step 2: 9-aminofluorene (0.43 g, 2.0 mmol) was added to a 250 mL round-bottom flask dissolved in 50 mL of toluene. The resulting solution was stirred for 10 min with a subsequent dropwise addition of benzoyl chloride (0.70 g, 5.0 mmol). The reaction was stirred for about 9 h. After it was filtered, the filtrate, a white solid, was obtained and washed with anhydrous ether. Yield: 0.46 g, 71%. <sup>1</sup>H NMR (400 MHz, *d*<sub>6</sub>-DMSO, TMS): δ 9.08 (d, *J* = 8.0 Hz, 1 H, N-H), 7.96 (d, *J* = 8.0 Hz, 2 H, Ar-H), 7.91 (d, *J* = 8.0 Hz, 2 H, Ar-H), 7.52 (d, *J* = 8.0 Hz, 3 H, Ar-H), 7.48–7.42 (m, 4 H, Ar-H), 7.33 (d, *J* = 8.0 Hz, 2 H, Ph-H), 5.40 (s, 1 H, C-H); <sup>13</sup>C NMR (100 MHz, *d*<sub>6</sub>-DMSO, TMS): 167.5, 145.2, 140.5, 131.7, 130.0, 128.6, 128.2, 127.9, 126.2, 125.1, 120.9, 120.5, 55.0.

**Synthesis of *N*-(anthracen-9-yl)benzamide (L9):** Step 1: the suspension of 9-nitroanthracene (0.11 g, 0.50 mmol) in glacial acetic acid (4 mL) was heated at 80 °C for 1.5 h. To the resulting homogeneous solution, a slurry of anhydrous SnCl<sub>2</sub> (0.49 g, 2.5 mmol) in conc. HCl (2 mL) was added via a dropping funnel over 10 min at 80 °C and the mixture was stirred for 2 h at 80 °C. The precipitate was filtered and washed with conc. HCl (3 × 20 mL). The solid was washed with 5% aq. NaOH and washed with sufficient water. The orange solid was dried in air shortly and at 50 °C in vacuo for 6 h. The product was obtained as orange

powder (0.65 g, 67%).  $^1\text{H}$  NMR (400 MHz,  $d_6$ -DMSO, TMS):  $\delta$  7.98–7.92 (m, 4 H), 7.88 (s, 1 H), 7.45–7.39 (m, 4 H)

Step 2: 9-aminoanthracene (0.038 g, 0.20 mmol) was added to a 50 mL round-bottom flask and dissolved in 20 mL of toluene. The resulting solution was stirred for 10 min with a subsequent dropwise addition of benzoyl chloride (0.084 g, 0.6 mmol). The reaction was stirred for about 12 h at 120 °C. After filtration, a yellow solid was obtained, and washed with anhydrous diethyl ether. Yield: 0.031 g, 52%.  $^1\text{H}$  NMR (400 MHz,  $d_6$ -DMSO, TMS):  $\delta$  10.75 (s, 1 H, N-H), 8.88 (d,  $J$  = 8.0 Hz, 2 H, Ph-H), 8.76 (d,  $J$  = 8.0 Hz, 2 H, Ar-H), 8.63–8.45 (m, 3 H, Ph-H), 8.08–8.01 (m, 7 H, Ar-H);  $^{13}\text{C}$  NMR (100 MHz,  $d_6$ -DMSO, TMS): 167.7, 139.9, 134.2, 132.1, 128.8, 128.2, 127.5, 125.4, 124.9, 122.1, 118.0, 117.2.

**Synthesis of *N*-(Pyrene-1-yl)benzamide (L10):** 1-pyrenamine (0.11 g, 0.50 mmol) was added to a 50 mL round-bottom flask and dissolved in 20 mL of toluene. The resulting solution was stirred for 10 min with a subsequent dropwise addition of benzoyl chloride (0.21 g, 1.5 mmol). The reaction was stirred for about 12 h at 120 °C. After filtration, a white solid was obtained, and it was washed with anhydrous diethyl ether. Yield: 0.03 g, 27%.  $^1\text{H}$  NMR (400 MHz,  $d_6$ -DMSO, TMS):  $\delta$  8.14 (d,  $J$  = 8.0 Hz, 4 H), 7.94 (d,  $J$  = 8.0 Hz, 2H), 7.81 (t,  $J$  = 8.0 Hz, 2 H, Ph-H), 7.66–7.60 (m, 4 H, Ar-H), 7.49 (t,  $J$  = 8.0 Hz, 2H, Ph-H);  $^{13}\text{C}$  NMR (100 MHz,  $d_6$ -DMSO, TMS): 166.7, 134.2, 132.1, 128.8, 127.7, 127.5, 122.5, 121.2.

### 3.3. Synthesis of Potassium Complexes

**Synthesis of *N*-(naphthalen-1-yl)benzamide potassium (K1):** The *N*-(naphthalen-1-yl)benzamide **L1** (0.25 g, 1.0 mmol) and potassium tert-butoxide (0.22 g, 2 mmol) was added into 20 mL tetrahydrofuran, and then the mixture was stirred for 12 h at room temperature. After that, the mixture was concentrated and *n*-hexane was added to precipitate the compounds. The white precipitate was obtained and washed with toluene and diethyl ether. The final product **K1** (0.22 g, 0.75 mmol) was obtained as a white solid in a yield 75%.  $^1\text{H}$  NMR (400 MHz,  $d_6$ -DMSO, TMS):  $\delta$  8.72 (d,  $J$  = 8.0 Hz, 1 H), 8.25 (d,  $J$  = 8.0 Hz, 2 H), 8.13 (d,  $J$  = 8.0 Hz, 1 H), 7.62 (d,  $J$  = 8.0 Hz, 1 H), 7.30–7.20 (m, 6 H), 7.07 (d,  $J$  = 8.0 Hz, 1 H);  $^{13}\text{C}$  NMR (100 MHz,  $d_6$ -DMSO, TMS): 165.6, 150.5, 144.2, 133.8, 130.8, 127.8, 126.8, 126.4, 126.3, 125.1, 123.8, 121.8, 116.3, 115.4.

**Synthesis of *N*-(4-bromonaphthalen-1-yl)benzamide potassium (K2):** The *N*-(4-bromonaphthalen-1-yl)benzamide **L2** (0.33 g, 1.0 mmol) and potassium tert-butoxide (0.22 g, 2.0 mmol) was added into 15 mL tetrahydrofuran, and then the mixture was stirred for 12 h at room temperature. After that, the mixture was concentrated and *n*-hexane was added to precipitate the compounds. The white precipitate was obtained and washed with toluene and diethyl ether. The final product **K2** (0.29 g, 0.79 mmol) was obtained as white solid in a yield of 79%.  $^1\text{H}$  NMR (400 MHz,  $d_6$ -DMSO, TMS):  $\delta$  8.78 (d,  $J$  = 8.0 Hz, 1 H), 8.24–8.21 (m, 2 H), 8.15 (d,  $J$  = 8.0 Hz, 1H), 7.92 (d,  $J$  = 8.0 Hz, 1 H), 7.57–7.49 (m, 2 H), 7.42–7.31 (m, 4 H);  $^{13}\text{C}$  NMR (100 MHz,  $d_6$ -DMSO, TMS): 167.1, 148.8, 142.9, 132.8, 132.0, 130.5, 128.4, 127.3, 126.6, 126.0, 125.6, 123.9, 118.6, 109.1.

**Synthesis of *N*-(4-nitronaphthalen-1-yl)benzamide potassium K3):** The *N*-(4-nitronaphthalen-1-yl) benzamide **L3** (0.29 g, 1.0 mmol) and potassium tert-butoxide (0.22 g, 2.0 mmol) was added into 15 mL tetrahydrofuran, and then the mixture was stirred 12 h at room temperature. After that, the mixture was concentrated and *n*-hexane was added to precipitate the compounds. The white precipitate was obtained and washed with toluene and diethyl ether. The final product **K2** (0.21 g, 0.72 mmol) was obtained as black solid in a yield of 72%.  $^1\text{H}$  NMR (400 MHz,  $d_6$ -DMSO, TMS):  $\delta$  8.90 (d,  $J$  = 8.0 Hz, 1 H), 8.86–8.84 (m, 2 H), 8.75 (d,  $J$  = 8.0 Hz, 1 H), 8.64 (s, 1 H), 8.25–8.23 (m, 1 H), 7.82–7.75 (m, 4H), 7.53 (t,  $J$  = 8.0 Hz, 1 H), 7.33 (t,  $J$  = 8.0 Hz, 3 H);  $^{13}\text{C}$  NMR (100 MHz,  $d_6$ -DMSO, TMS): 159.1, 148.5, 132.6, 131.0, 130.9, 130.0, 129.4, 128.9, 128.2, 127.6, 127.3, 126.2, 124.9, 124.3, 124.1, 124.0, 110.9.

**Synthesis of *N*-(dibenzhydrylnaphthalen-1-yl) benzamide potassium (K4):** The *N*-(dibenzhydrylnaphthalen-1-yl)benzamide **L4** (0.30 g, 1.0 mmol) and potassium tert-butoxide (0.22 g, 2.0 mmol) was added into 30 mL tetrahydrofuran, and then the mixture was stirred

for 12 h at room temperature. After concentration, the *n*-hexane was added to precipitate the compounds. The white precipitate was obtained and washed with dichloromethane and diethyl ether. The final product **K4** (0.30 g, 0.77 mmol) was obtained as a white solid in a yield of 77%. <sup>1</sup>H NMR: (400 MHz, *d*<sub>6</sub>-DMSO, TMS): δ 8.77 (s, 1 H), 8.21 (d, *J* = 8.0 Hz, 2 H), 7.95 (t, *J* = 8.0 Hz, 1 H), 7.81 (d, *J* = 8.0 Hz, 1 H), 7.31–18 (m, 11 H), 7.13 (d, *J* = 8.0 Hz, 4 H), 6.64 (d, *J* = 8.0 Hz, 1 H), 6.20 (s, 1 H). <sup>13</sup>C NMR (100 MHz, *d*<sub>6</sub>-DMSO, TMS): 166.4, 145.1, 132.6, 129.8, 128.6, 128.0, 127.3, 126.4, 126.2, 125.1, 123.7, 122.8, 52.5.

**Synthesis of 4-methyl-*N*-(naphthalen-1-yl) benzamide potassium (K5):** The 4-methyl-*N*-(naphthalen-1-yl)benzamide **L5** (0.50 g, 2.0 mmol) and potassium tert-butoxide (0.44 g, 4.0 mmol) was added into 30 mL of tetrahydrofuran, and then the mixture was stirred for 12 h at room temperature. After concentration, the *n*-hexane was added to precipitate the compounds. The white precipitate was obtained and washed with dichloromethane and diethyl ether. The final product **K5** (0.30 g, 1.12 mmol) was obtained as a white solid in yield of 56%. <sup>1</sup>H NMR: (400 MHz, *d*<sub>6</sub>-DMSO, TMS): δ 8.38 (s, 1 H), 8.08 (s, 2 H), 7.89 (s, 1H), 7.77 (s, 1 H), 7.37 (s, 4 H), 7.21 (s, 2 H). <sup>13</sup>C NMR (100 MHz, *d*<sub>6</sub>-DMSO, TMS): 166.5, 134.5, 130.6, 128.6, 128.5, 127.9, 126.4, 125.6, 124.8, 124.6, 21.5.

**Synthesis of 4-methoxy-*N*-(naphthalen-1-yl) benzamide potassium (K6):** The 4-methoxy-*N*-(naphthalen-1-yl)benzamide **L6** (0.50 g, 2.0 mmol) and potassium tert-butoxide (0.44 g, 4.0 mmol) was added into 30 mL of tetrahydrofuran, and then the mixture was stirred for 12 h at room temperature. After concentration, the *n*-hexane was added to precipitate the compounds. The white precipitate was obtained and washed with dichloromethane and diethyl ether. The final product **K6** (0.39 g, 1.32 mmol) was obtained as a white solid in a yield of 65%. <sup>1</sup>H NMR: (400 MHz, *d*<sub>6</sub>-DMSO, TMS): δ 8.57 (d, *J* = 8 Hz, 1 H), 8.15 (d, *J* = 8 Hz, 2H), 8.02 (d, *J* = 8 Hz, 1 H), 7.65 (d, *J* = 8 Hz, 1 H), 7.32–22 (m, 2 H), 7.17 (d, *J* = 8 Hz, 1 H), 6.86 (d, *J* = 8 Hz, 2 H). <sup>13</sup>C NMR: (100 MHz, *d*<sub>6</sub>-DMSO, TMS): δ 163.4, 163.2, 161.6, 132.2, 131.7, 131.4, 131.0, 130.7, 129.3, 128.1, 126.5, 126.3, 126.0, 125.4, 124.4, 123.8, 116.1, 112.9.

**Synthesis of 4-fluoro-*N*-(naphthalen-1-yl) benzamide potassium (K7):** The 4-fluoro-*N*-(naphthalen-1-yl)benzamide **L7** (0.60 g, 2.0 mmol) and potassium tert-butoxide (0.44 g, 4.0 mmol) was added into 30 mL of tetrahydrofuran, and then the mixture was stirred for 12 h at room temperature. After concentration, the *n*-hexane was added to precipitate the compounds. The white precipitate was obtained and washed with dichloromethane and diethyl ether. The final product **K7** (0.40 g, 1.34 mmol) was obtained as a white solid in a yield of 67%. <sup>1</sup>H NMR: (400 MHz, *d*<sub>6</sub>-DMSO, TMS): δ 8.71 (d, *J* = 8 Hz, 1 H), 8.30–8.27 (m, 2 H), 8.15 (d, *J* = 8 Hz, 1 H), 7.63 (d, *J* = 8 Hz, 1 H), 7.30–7.21 (m, 3 H), 7.11–7.06 (d, 3 H); <sup>13</sup>C NMR: (100 MHz, *d*<sub>6</sub>-DMSO, TMS): δ 165.8, 165.5, 163.4, 134.2, 131.4, 131.3, 131.0, 130.9, 129.7, 128.5, 126.8, 126.5, 126.4, 125.9, 124.4, 123.8, 115.9, 115.7.

**Synthesis of *N*-(9H-fluoren-9-yl)benzamide potassium (K8):** The *N*-(9H-fluoren-9-yl)benzamide **L8** (0.28 g, 1.0 mmol) and potassium tert-butoxide (0.22 g, 2.0 mmol) was added into 20 mL tetrahydrofuran, and then the mixture was stirred for 9 h at room temperature. After that, the mixture was concentrated and *n*-hexane was added to precipitate the compounds. The white precipitate was obtained and washed with toluene and diethyl ether. The final product **K8** (0.26 g, 0.82 mmol) was obtained as a white solid in a yield of 82%. <sup>1</sup>H NMR (400 MHz, *d*<sub>6</sub>-DMSO, TMS): δ 8.06 (d, *J* = 8.0 Hz, 1 H), 7.94 (t, *J* = 4.0 Hz, 1 H), 7.86 (d, *J* = 8.0 Hz, 2 H), 7.52 (d, *J* = 8.0 Hz, 2 H), 7.44–7.37 (m, 2 H), 7.29–7.11 (m, 4 H), 6.83 (s, 1 H), 6.47 (s, 1 H); <sup>13</sup>C NMR (100 MHz, *d*<sub>6</sub>-DMSO, TMS): 166.1, 128.4, 128.1, 127.2, 124.2, 120.2, 114.0, 113.8, 55.1.

**Synthesis of *N*-(anthracen-9-yl)benzamide potassium (K9):** the *N*-(anthracen-9-yl)benzamide **L9** (0.30 g, 1 mmol) and potassium tert-butoxide (0.22 g, 2.0 mmol) was added into 20 mL of tetrahydrofuran, and then the mixture was stirred for 12 h at room temperature. After that, the mixture was concentrated and *n*-hexane was added to precipitate the compounds. The white precipitate was obtained and washed with toluene and diethyl ether. The final product **K9** (0.26 g, 0.82 mmol) was obtained as a yellow solid in a yield of 82%. <sup>1</sup>H NMR (400 MHz, *d*<sub>6</sub>-DMSO, TMS): δ 8.56 (s, 4 H), 8.24 (d, *J* = 8.0 Hz, 2 H), 8.17 (d,

$J = 8.0$  Hz, 2 H), 7.82 (d,  $J = 8.0$  Hz, 2 H), 7.29 (t,  $J = 8.0$  Hz, 1 H), 7.11 (d,  $J = 8.0$  Hz, 2 H);  $^{13}\text{C}$  NMR (100 MHz,  $d_6$ -DMSO, TMS): 167.1, 153.8, 144.1, 128.5, 127.4, 127.1, 125.7, 120.4, 125.4, 55.4

**Synthesis of *N*-(Pyrene-1-yl)benzamide potassium (K10):** The *N*-(Pyrene-1-yl)benzamide **L10** (0.32 g, 1.0 mmol) and potassium tert-butoxide (0.22 g, 2.0 mmol) was added into 20 mL of tetrahydrofuran, and then the mixture was stirred for 12 h at room temperature. After that, the mixture was concentrated and *n*-hexane was added to precipitate the compounds. The white precipitate was obtained and washed with toluene and diethyl ether. The final product **K10** (0.28 g, 0.83 mmol) was obtained as a yellow solid in a yield of 83%.  $^1\text{H}$  NMR (400 MHz,  $d_6$ -DMSO, TMS):  $\delta$  8.93 (d,  $J = 8.0$  Hz, 1 H), 8.78 (d,  $J = 8.0$  Hz, 1 H), 8.33 (d,  $J = 8.0$  Hz, 2 H), 7.93–7.86 (m, 4 H), 7.81–7.78 (m, 2 H), 7.68 (d,  $J = 8.0$  Hz, 1H), 7.36–7.30 (m, 3 H);  $^{13}\text{C}$  NMR (100 MHz,  $d_6$ -DMSO, TMS): 167.0, 132.1, 132.0, 129.1, 128.5, 128.1, 127.9, 127.2, 125.8, 125.6, 124.3, 123.1, 122.4, 122.3, 122.1, 122.0.

### 3.4. General Procedure for the ROP of *L*-LA and *rac*-LA

All procedures using *L*-LA as the monomer were similar; a typical polymerization was detailed as follows, using **K2** as the representative precatalyst. Complex **K2** (20  $\mu\text{mol}$ ) was introduced to a Schlenk flask and a toluene solution of benzyl alcohol (0.2 mL, 100  $\mu\text{mol}/\text{mL}$  in toluene). The reaction mixture was stirred at room temperature for 5 min before the flask was placed in a temperature-controlled oil bath preheated to the designated temperature, and *L*-LA (0.72 g, 5.00 mmol) and toluene (0.8 mL) was promptly injected. After the mixture was stirred for the designated time, the resulting viscous solution was transferred into a beaker containing cold methanol (100 mL) and stirred. The resulting polymer was collected on filter paper and dried under reduced pressure to provide the PLLA as a white solid. The polymerizations using *rac*-LA as a monomer were conducted in a similar manner to that described for *L*-LA.

### 3.5. Crystal Structure Determination

Single crystals of **K2** and **K10** suitable for X-ray structural analysis were grown from a mixture of THF and *n*-hexane at room temperature. The single crystal X-ray diffraction studies was performed on a Rigaku RAXIS Rapid IP diffractometer with graphite monochromated Cu-K $\alpha$  radiation ( $\lambda = 1.54184$  Å) at 170(10) K. Reflections were merged by SHELXL according to the crystal class for the calculation of statistics and refinement [68]. Intensities were corrected for Lorentz and polarization effects and empirical absorption. The structures were solved by direct methods and refined by full matrix least-squares on  $F^2$ . All non-hydrogen atoms were refined anisotropically. Structure solution was performed by using the OLEX2.solve, and refinement was performed by using the SHELXL package [69,70]. Details of the X-ray structure determination and refinement are provided in Table S1.

## 4. Conclusions

In summary, a series of potassium amidate complexes **K1–K10** were prepared and characterized by  $^1\text{H}/^{13}\text{C}$  NMR. The crystal structure of **K2**, **K10** showed that the interaction between K and aryl ring generated a “CpM” form. All potassium complexes exhibited high catalytic activity towards ring-opening polymerization of *L*-lactide, and the substituent greatly affected their activity. When the molar ratio of [LA]:[K] was 500, at 50 °C, in the presence of BnOH, the monomer conversion by these potassium complexes **K1–K10** is higher than 70% within 10 min, and the monomer conversion could reach 96% within 15 min. The structural analysis of the obtained PLLA shows that all of them had a linear structure with CH<sub>3</sub>O- as the end group. In addition, these potassium complexes exhibited moderate to good selectivity, with  $P_m$  ranging from 0.56 to 0.76 for ROP of *rac*-LA, and substituent on the ligand and the reaction time greatly affected the monomer conversion and isoselectivities.

**Supplementary Materials:** The following supporting information can be downloaded at: <https://www.mdpi.com/article/10.3390/catal13040770/s1>, Figures display the NMR spectra of potassium complexes as well as Homonuclear-decoupled  $^1\text{H}$  NMR spectroscopy of polymer of ROP of *rac*-LA by different potassium complexes. X-ray crystallographic CIF files for CCDC 2244714 (**K2**), 2244715 (**K10**) are available free of charge from the Cambridge Crystallographic Data Centre. See supporting information.

**Author Contributions:** Design of the study by W.Z.; synthesis of the organic compounds and the potassium complexes by J.G.; characterization by J.G. and X.W.; X-ray study by M.H. and X.H.; catalytic study by J.G.; characterization of polymer by J.G., F.C. and R.W.; writing and editing by W.Z. and J.G. All authors have read and agreed to the published version of the manuscript.

**Funding:** This research was funded by the National Natural Science Foundation of China (51973005) and Beijing Scholar Program (Project No. RCQJ20303).

**Data Availability Statement:** Not applicable.

**Conflicts of Interest:** The authors declare no conflict of interest.

## References

1. Iwata, T. Biodegradable and Bio-Based Polymers: Future Prospects of Eco-Friendly Plastics. *Angew. Chem. Int. Ed.* **2015**, *54*, 3210–3215. [[CrossRef](#)] [[PubMed](#)]
2. Zhang, X.; Fevre, M.; Jones, G.O.; Waymouth, R.M. Catalysis as an Enabling Science for Sustainable Polymers. *Chem. Rev.* **2018**, *118*, 839–885. [[CrossRef](#)] [[PubMed](#)]
3. Schwach, G.; Coudane, J.; Engel, R.; Vert, M. Zn lactate as initiator of DL-lactide ring opening polymerization and comparison with Sn octoate. *Poly. Bull.* **1996**, *37*, 771–776. [[CrossRef](#)]
4. Wu, J.; Yu, T.L.; Chen, C.T.; Lin, C.C. Recent developments in main group metal complexes catalyzed/initiated polymerization of lactides and related cyclic esters. *Coord. Chem. Rev.* **2006**, *250*, 602–626. [[CrossRef](#)]
5. Cabaret, O.D.; Vaca, B.M.; Bourissou, D. Controlled Ring-Opening Polymerization of Lactide and Glycolide. *Chem. Rev.* **2004**, *104*, 6147–6176. [[CrossRef](#)]
6. Guillaume, S.M.; Kirillov, E.; Sarazin, Y.; Carpentier, J.F. Beyond Stereoselectivity, Switchable Catalysis: Some of the Last Frontier Challenges in Ring-Opening Polymerization of Cyclic Esters. *Chem. Eur. J.* **2015**, *21*, 7988–8003. [[CrossRef](#)]
7. Sarazin, Y.; Carpentier, J.-F. Discrete Cationic Complexes for Ring-Opening Polymerization Catalysis of Cyclic Esters and Epoxides. *Chem. Rev.* **2015**, *115*, 3564–3614. [[CrossRef](#)] [[PubMed](#)]
8. Santoro, O.; Zhang, X.; Redshaw, C. Synthesis of Biodegradable Polymers: A Review on the Use of Schiff-Base Metal Complexes as Catalysts for the Ring Opening Polymerization (ROP) of Cyclic Esters. *Catalysts* **2020**, *10*, 800. [[CrossRef](#)]
9. Wu, L.-J.; Lee, W.; Ganta, P.K.; Chang, Y.-L.; Chang, Y.-C.; Chen, H.-Y. Multinuclear metal catalysts in ring-opening polymerization of  $\epsilon$ -caprolactone and lactide: Cooperative and electronic effects between metal centers. *Coord. Chem. Rev.* **2023**, *475*, 214847. [[CrossRef](#)]
10. Lyubov, D.M.; Tolpygin, A.O.; Trifonov, A.A. Rare-earth metal complexes as catalysts for ring-opening polymerization of cyclic esters. *Coord. Chem. Rev.* **2019**, *392*, 83–145. [[CrossRef](#)]
11. Strianese, M.; Pappalardo, D.; Mazzeo, M.; Lamberti, M.; Pellicchia, C. Salen-type aluminum and zinc complexes as two faced Janus compounds: Contribution to molecular sensing and polymerization catalysis. *Dalton Trans.* **2020**, *49*, 16533–16550. [[CrossRef](#)] [[PubMed](#)]
12. Gadowska-Gajadhur, A.; Ruśkowski, P. Biocompatible Catalysts for Lactide Polymerization Catalyst Activity, Racemization Effect, and Optimization of the Polymerization Based on Design of Experiments. *Org. Process Res. Dev.* **2020**, *24*, 1435–1442. [[CrossRef](#)]
13. Chen, M.; Chen, C. Controlling the Ring-Opening Polymerization Process Using External Stimuli. *Chin. J. Chem.* **2020**, *38*, 282–286. [[CrossRef](#)]
14. Kaler, S.; Jones, M.D. Recent advances in externally controlled ring-opening polymerisations. *Dalton Trans.* **2022**, *51*, 1241–1256. [[CrossRef](#)]
15. Kricheldorf, H.R.; Weidner, S.M. Syntheses of polylactides by means of tin catalysts. *Polym. Chem.* **2022**, *13*, 1618–1647. [[CrossRef](#)]
16. Farah, S.; Anderson, D.G.; Langer, R. Physical and mechanical properties of PLA, and their functions in widespread applications—A comprehensive review. *Adv. Drug Deliver. Rev.* **2016**, *107*, 367–392. [[CrossRef](#)]
17. Lima, L.-T.; Aurasb, R.; Rubinob, M. Processing technologies for poly(lactic acid). *Prog. Poly. Sci.* **2008**, *33*, 820–852. [[CrossRef](#)]
18. Albertsson, A.-C.; Varma, I.K. Recent Developments in Ring Opening Polymerization of Lactones for Biomedical Applications. *Biomacromolecules* **2003**, *4*, 1466–1486. [[CrossRef](#)]
19. Auras, R.; Harte, B.; Selke, S. An Overview of Polylactides as Packaging Materials. *Macromol. Biosci.* **2004**, *4*, 835–864. [[CrossRef](#)]
20. Middleton, J.C.; Tipton, A.J. Synthetic biodegradable polymers as orthopedic devices. *Biomaterials* **2000**, *21*, 2335–2346. [[CrossRef](#)]

21. Oudega, M.; Gautier, S.E.; Chapon, P.; Fragoso, M.; Bates, M.L.; Parel, J.-M.; Bunge, M.B. Axonal regeneration into Schwann cell grafts within resorbable poly( $\alpha$ -hydroxyacid) guidance channels in the adult rat spinal cord. *Biomaterials* **2001**, *22*, 1125–1136. [[CrossRef](#)] [[PubMed](#)]
22. Wei, G.; Ma, P.X. Structure and properties of nano-hydroxyapatite/polymer composite scaffolds for bone tissue engineering. *Biomaterials* **2004**, *25*, 4749–4757. [[CrossRef](#)] [[PubMed](#)]
23. Ikada, Y.; Jamshidi, K.; Tsuji, H.; Hyon, S.-H. Stereocomplex formation between enantiomeric poly(lactides). *Macromolecules* **1987**, *20*, 904–906. [[CrossRef](#)]
24. Stanford, M.J.; Dove, A.P. Stereocontrolled ring-opening polymerisation of lactide. *Chem. Soc. Rev.* **2010**, *39*, 486–494. [[CrossRef](#)]
25. Thomas, C.M. Stereocontrolled ring-opening polymerization of cyclic esters: Synthesis of new polyester microstructures. *Chem. Soc. Rev.* **2010**, *39*, 165–173. [[CrossRef](#)]
26. Dijkstra, P.J.; Du, H.; Feijen, J. Single site catalysts for stereoselective ring-opening polymerization of lactides. *Polym. Chem.* **2011**, *2*, 520–527. [[CrossRef](#)]
27. Kowalski, A.; Duda, A.; Penczek, S. Mechanism of Cyclic Ester Polymerization Initiated with Tin(II) Octoate. 2. Macromolecules Fitted with Tin(II) Alkoxide Species Observed Directly in MALDI–TOF Spectra. *Macromolecules* **2000**, *33*, 689–695. [[CrossRef](#)]
28. Dove, A.P.; Gibson, V.C.; Marshall, E.L.; Rzepa, H.S.; White, A.J.P.; Williams, D.J. Synthetic, Structural, Mechanistic, and Computational Studies on Single-Site  $\beta$ -Diketiminato Tin(II) Initiators for the Polymerization of rac-Lactide. *J. Am. Chem. Soc.* **2006**, *128*, 9834–9843. [[CrossRef](#)]
29. Kremer, A.B.; Mehrkhodavandi, P. Dinuclear catalysts for the ring opening polymerization of lactide. *Coord. Chem. Rev.* **2019**, *380*, 35–37. [[CrossRef](#)]
30. Carpentier, J.-F. Rare-Earth Complexes Supported by Tripodal Tetradentate Bis(phenolate) Ligands: A Privileged Class of Catalysts for Ring-Opening Polymerization of Cyclic Esters. *Organometallics* **2015**, *34*, 4175–4189. [[CrossRef](#)]
31. Marin, P.; Venditto, V.; Thomas, C.M. Polymerization of rac-Lactide Using Achiral Iron Complexes: Access to Thermally Stable Stereocomplexes. *Angew. Chem. Int. Ed.* **2019**, *58*, 12585–12589. [[CrossRef](#)] [[PubMed](#)]
32. Pang, X.; Duan, R.; Li, X.; Hu, C.; Wang, X.; Chen, X. Breaking the Paradox between Catalytic Activity and Stereoselectivity: Rac-Lactide Polymerization by Trinuclear Salen–Al Complexes. *Macromolecules* **2018**, *51*, 906–913. [[CrossRef](#)]
33. Ren, F.; Li, X.; Xian, J.; Han, X.; Cao, L.; Pan, X.; Wu, J. Bench-stable potassium complexes for living and isoselective ring-opening polymerization of rac-lactide. *J. Polym. Sci.* **2022**, *60*, 2847–2854. [[CrossRef](#)]
34. Katalin, D.-P.; Oldenburg, F.J.; Menzel, J.P.; Springer, M.; Dawe, L.N.; Kozak, C.M. Lithium, sodium, potassium and calcium amine-bis(phenolate) complexes in the ring-opening polymerization of rac-lactide. *Dalton Trans.* **2020**, *49*, 1531–1544.
35. Spassky, N.; Wisniewski, M.; Pluta, C.; Borgne, A.L. Highly stereoselective polymerization of rac-(D, L)-lactide with a chiral Schiff's base/aluminium alkoxide initiator. *Macromol. Chem. Phys.* **1996**, *197*, 2627–2637. [[CrossRef](#)]
36. Meduri, A.; Fuoco, T.; Lamberti, M.; Pellicchia, C.; Pappalardo, D. Versatile Copolymerization of Glycolide and rac-Lactide by Dimethyl(salicylaldehyde)aluminum Compounds. *Macromolecules* **2014**, *47*, 534–543. [[CrossRef](#)]
37. Nomura, N.; Ishii, R.; Akakura, M.; Aoi, K. Stereoselective Ring-Opening Polymerization of Racemic Lactide Using Aluminum–Achiral Ligand Complexes: Exploration of a Chain-End Control Mechanism. *J. Am. Chem. Soc.* **2002**, *124*, 5938–5939. [[CrossRef](#)]
38. Hornmair, P.; Marshall, E.L.; Gibson, V.C.; White, A.J.P.; Williams, D.J. Remarkable Stereocontrol in the Polymerization of Racemic Lactide Using Aluminum Initiators Supported by Tetradentate Aminophenoxide Ligands. *J. Am. Chem. Soc.* **2004**, *126*, 2688–2689. [[CrossRef](#)]
39. Nomura, N.; Ishii, R.; Yamamoto, Y.; Kondo, T. Stereoselective Ring-Opening Polymerization of a Racemic Lactide by Using Achiral Salen–and Homosalen–Aluminum Complexes. *Chem. Eur. J.* **2007**, *13*, 4433–4451. [[CrossRef](#)]
40. Hornmair, P.; Marshall, E.L.; Gibson, V.C.; Pugh, R.I.; White, A.J.P. Study of ligand substituent effects on the rate and stereoselectivity of lactide polymerization using aluminum salen-type initiators. *Proc. Natl. Acad. Sci. USA* **2006**, *103*, 15343–15348. [[CrossRef](#)]
41. Tang, Z.; Chen, X.; Pang, X.; Yang, Y.; Zhang, X.; Jing, X. Stereoselective Polymerization of rac-Lactide Using a Monoethylaluminum Schiff Base Complex. *Biomacromolecules* **2004**, *5*, 965–970. [[CrossRef](#)] [[PubMed](#)]
42. Gao, J.; Zhu, D.; Zhang, W.; Solan, G.A.; Ma, Y.; Sun, W.-H. Recent progress in the application of group 1, 2 & 13 metal complexes as catalysts for the ring opening polymerization of cyclic esters. *Inorg. Chem. Front.* **2019**, *6*, 2619–2652.
43. Dai, Z.; Sun, Y.; Xiong, J.; Pan, X.; Wu, J. Alkali-Metal Monophenolates with a Sandwich-Type Catalytic Center as Catalysts for Highly Isoselective Polymerization of rac-Lactide. *ACS Macro Lett.* **2015**, *4*, 556–560. [[CrossRef](#)]
44. Sun, Y.; Xiong, J.; Dai, Z.; Pan, X.; Tang, N.; Wu, J. Stereoselective Alkali-Metal Catalysts for Highly Isotactic Poly(rac-lactide) Synthesis. *Inorg. Chem.* **2016**, *55*, 136–143. [[CrossRef](#)]
45. Dai, Z.; Sun, Y.; Xiong, J.; Pan, X.; Tang, N.; Wu, J. Simple sodium and potassium phenolates as catalysts for highly isoselective polymerization of rac-lactide. *Catal. Sci. Technol.* **2016**, *6*, 515–520. [[CrossRef](#)]
46. Wu, B.-B.; Tian, L.-L.; Wang, Z.-X. Ring-opening polymerization of rac-lactide catalyzed by crown ether complexes of sodium and potassium iminophenoxides. *RSC Adv.* **2017**, *7*, 24055–24063. [[CrossRef](#)]
47. Chen, C.; Cui, Y.; Mao, X.; Pan, X.; Wu, J. Suppressing Cyclic Polymerization for Isoselective Synthesis of High-Molecular-Weight Linear Polylactide Catalyzed by Sodium/Potassium Sulfonamidate Complexes. *Macromolecules* **2017**, *50*, 83–96. [[CrossRef](#)]
48. Wu, B.-B.; Wang, Z.-X. Crown ether complexes of potassium quinolin-8-olates: Synthesis, characterization and catalysis toward the ring-opening polymerization of rac-lactide. *RSC Adv.* **2017**, *7*, 11657–11664. [[CrossRef](#)]

49. Fernández-M, M.; Ortega, P.; Cuenca, T.; Cano, J.; Mosquera, M.E.G. Alkali-Metal Compounds with Bio-Based Ligands as Catalysts for Isoselective Lactide Polymerization: Influence of the Catalyst Aggregation on the Polymerization Control. *Organometallics* **2020**, *39*, 2278–2286. [[CrossRef](#)]
50. Zhang, J.; Xiong, J.; Sun, Y.; Tang, N.; Wu, J. Highly Iso-Selective and Active Catalysts of Sodium and Potassium Monophenoxides Capped by a Crown Ether for the Ring-Opening Polymerization of rac-Lactide. *Macromolecules* **2014**, *47*, 7789–7796. [[CrossRef](#)]
51. Chen, C.; Jiang, J.; Mao, X.; Cong, Y.; Cui, Y.; Pan, X.; Wu, J. Isoselective Polymerization of rac-Lactide Catalyzed by Ion-Paired Potassium Amidinate Complexes. *Inorg. Chem.* **2018**, *57*, 3158–3168. [[CrossRef](#)]
52. Yao, C.; Yang, Y.; Ma, H. Potassium complexes supported by monoanionic tetradentate amino-phenolate ligands: Synthesis, structure and catalysis in the ring-opening polymerization of rac-lactide. *Dalton Trans.* **2017**, *46*, 6087–6097. [[CrossRef](#)] [[PubMed](#)]
53. Zhang, Q.; Zhang, W.; Wang, S.; Solan, G.A.; Liang, T.; Rajendrana, N.M.; Sun, W.-H. Sodium iminoquinolates with cubic and hexagonal prismatic motifs: Synthesis, characterization and their catalytic behavior toward the ROP of rac-lactide. *Inorg. Chem. Front.* **2016**, *3*, 1178–1189. [[CrossRef](#)]
54. Gao, J.; Zhang, W.; Cao, F.; Solan, G.A.; Zhang, X.; Jiang, Y.; Hao, X.; Sun, W.-H. Potassium N-arylbenzimidates as readily accessible and benign (pre)catalysts for the ring opening polymerization of  $\epsilon$ -CL and L-LA. *Mol. Catal.* **2020**, *498*, 111280. [[CrossRef](#)]
55. Montaudo, G.; Montaudo, M.S.; Puglisi, C.; Samperi, F.; Spassky, N.; LeBorgne, A.; Wisniewski, M. Evidence for Ester-Exchange Reactions and Cyclic Oligomer Formation in the Ring-Opening Polymerization of Lactide with Aluminum Complex Initiators. *Macromolecules* **1996**, *29*, 6461–6465. [[CrossRef](#)]
56. Spassky, N.; Simic, V.; Montaudo, M.S.; Hubert-Pfalzgraf, L.G. Inter- and intramolecular ester exchange reactions in the ring-opening polymerization of (D,L)-lactide using lanthanide alkoxide initiators. *Macromol. Chem. Phys.* **2000**, *201*, 2432–2440. [[CrossRef](#)]
57. Save, M.; Schappacher, M.; Soum, A. Controlled Ring-Opening Polymerization of Lactones and Lactides Initiated by Lanthanum Isopropoxide, 1. General Aspects and Kinetics. *Macromol. Chem. Phys.* **2002**, *203*, 889–899. [[CrossRef](#)]
58. Iwasa, N.; Katao, S.; Liu, J.; Fujiki, M.; Furukawa, Y.; Nomura, K. Notable Effect of Fluoro Substituents in the Imino Group in Ring-Opening Polymerization of  $\epsilon$ -Caprolactone by Al Complexes Containing Phenoxyimine Ligands. *Organometallics* **2009**, *28*, 2179–2187. [[CrossRef](#)]
59. Cayuela, J.; Bounor-Legaré, V.; Cassagnau, P.; Michel, A. Ring-Opening Polymerization of  $\epsilon$ -Caprolactone Initiated with Titanium n-Propoxide or Titanium Phenoxide. *Macromolecules* **2006**, *39*, 1338–1346. [[CrossRef](#)]
60. Baran, J.; Duda, A.; Kowalski, A.; Szymanski, R.; Penczek, S. Intermolecular chain transfer to polymer with chain scission: General treatment and determination of  $k_p/k_{tr}$  in L, L-lactide polymerization. *Macromol. Rapid Commun.* **1997**, *18*, 325–333. [[CrossRef](#)]
61. Huang, B.-H.; Ko, B.-T.; Athar, T.; Lin, C.-C. Synthesis, Characterization, and Structural Determination of Polynuclear Lithium Aggregates and Factors Affecting Their Aggregation. *Inorg. Chem.* **2006**, *45*, 7348–7356. [[CrossRef](#)]
62. Maudoux, N.; Roisnel, T.; Carpentier, J.-F.; Sarazin, Y. Aluminum, Indium, and Mixed Yttrium–Lithium Complexes Supported by a Chiral Binap-Based Fluorinated Dialkoxide: Structural Features and Heteroselective ROP of Lactide. *Organometallics* **2014**, *33*, 5740–5748. [[CrossRef](#)]
63. García-Valle, F.M.; Estivill, R.; Gallegos, C.; Cuenca, T.; Mosquera, M.E.G.; Taberero, V.; Cano, J. Metal and Ligand-Substituent Effects in the Immortal Polymerization of rac-Lactide with Li, Na, and K Phenoxo-imine Complexes. *Organometallics* **2015**, *34*, 477–487. [[CrossRef](#)]
64. Roşca, S.-C.; Roşca, D.-A.; Dorcet, V.; Kozak, C.M.; Kerton, F.M.; Carpentier, J.-F.; Sarazin, Y. Alkali aminoether-phenolate complexes: Synthesis, structural characterization and evidence for an activated monomer ROP mechanism. *Dalton Trans.* **2013**, *42*, 9361–9375. [[CrossRef](#)] [[PubMed](#)]
65. Gallegos, C.; Taberero, V.; Mosquera, M.E.G.; Cuenca, T.; Cano, J. Comparative Study of Lactide Polymerization with Lithium, Sodium, Potassium, Magnesium, Calcium, and Zinc Azo naphthoxide Complexes. *Eur. J. Inorg. Chem.* **2015**, *30*, 5124–5132. [[CrossRef](#)]
66. Cui, Y.; Chen, C.; Sun, Y.; Wu, J.; Pan, X. Isoselective mechanism of the ring-opening polymerization of rac-lactide catalyzed by chiral potassium binolates. *Inorg. Chem. Front.* **2017**, *4*, 261–269. [[CrossRef](#)]
67. Stirling, E.; Champouret, Y.; Viseaux, M. Catalytic metal-based systems for controlled statistical copolymerisation of lactide with a lactone. *Polym. Chem.* **2018**, *9*, 2517–2531. [[CrossRef](#)]
68. Sheldrick, G.M. Crystal structure refinement with SHELXL. *Acta Cryst.* **2015**, *C71*, 3–8.
69. Bourhis, L.J.; Dolomanov, O.V.; Gildea, R.J.; Howard, J.A.K.; Puschmann, H. The anatomy of a comprehensive constrained, restrained refinement program for the modern computing environment—Olex2 dissected. *Acta Cryst.* **2015**, *A71*, 59–75.
70. Dolomanov, O.V.; Bourhis, L.J.; Gildea, R.J.; Howard, J.A.K.; Puschmann, H. OLEX<sub>2</sub>: A complete structure solution, refinement and analysis program. *J. Appl. Cryst.* **2009**, *42*, 339–341. [[CrossRef](#)]

**Disclaimer/Publisher’s Note:** The statements, opinions and data contained in all publications are solely those of the individual author(s) and contributor(s) and not of MDPI and/or the editor(s). MDPI and/or the editor(s) disclaim responsibility for any injury to people or property resulting from any ideas, methods, instructions or products referred to in the content.